SYNCHRONIZING CONTROL OF A TWIN AXES TABLE DRIVE

LEE DAI JIN

BACHELOR OF ELCTRICAL ENGINEERING

(CONTROL, INSTRUMENTATION AND AUTOMATION)

UNIVERSITI TEKNIKAL MALAYSIA MELAKA

"I hereby declare that I have read through this report entitled "Synchronizing Control On A Twin Axes Table Drive" and found that it complies the partial fulfillment for awarding the degree of Bachelor of Electrical Engineering"

Signature : ----------

Supervisor's Name : PROF. MADYA. DR. CHONG SHIN HORNG

Date : _____

SYNCHRONIZING CONTROL OF A TWIN AXES TABLE DRIVE

LEE DAI JIN

A report submitted in partial fulfillment of the requirements for the degree of Bachelor of Electrical Engineering.

Faculty Of Electrical Engineering

UNIVERSITI TEKNIKAL MALAYSIA MELAKA

2018

I declare that this report entitled "*Synchronizing Control of A Twin Axes Table Drive*" is the result of my own research except as cited in the references. The report has not been accepted for any degree and is not concurrently submitted in candidature of any other degree.

Signature : .....

Name : LEE DAI JIN

Date : .....

To my beloved mother and father,

I would like to thank for the supports and the loves given to me which accompanied me to get through all obstacles and difficulties.

ACKNOWLEDGEMENT

In preparing this report, I was in contact with a lot of people, academicians, lecturers and friends. They have contributed towards my understanding and my thoughts about the final year project I am on to. I would like to express my sincere appreciation to my main supervisor, Professor Madya Dr, Chong Shin Horng, for the guidance, critics, and encouragement. I am also very thankful to my colleagues, Lim Vun Haw who contributes much in helping of the project hardware construction and advices given by him. I woud also like to thank for the panels, Dr. Azrita Alias and En. Muhamad Khairi Aripin for their guidance, advices and motivation. Without their continued support, this project would not have been same as presented here.

My sincere appreciation also extends to all my colleagues and others who have aided at various situations. Their helps are useful indeed. However, it is not possible to list all them in this limited space. I am lastly grateful to all my family members.

ABSTRACT

Twin axes drive table is an application that widely used in carriage purpose and industry. A synchronous control is used for efficient driving on the twin axes drive table which simultaneously driven by two separated DC linear motor. Position error tracking becomes the most important part to be observed in synchronous twin axes drive table. At relatively high velocity, the twin axes drive table needed to obtain zero synchronous error in term of position for both axes. Moreover, synchronization on the mechanically coupled twin axes table is the main challenge as damages may occurs when synchronization failed. This project is aimed to obtain and validate an accurate modelling transfer function by kinematical mathematical wise with an experiment. The modelling transfer function need to be accurate as the accuracy of the modelling transfer function affect a lot on the design of synchronous controller. Besides, this project is aimed to propose a classical PID controller that approximate to zero synchronous errors with simulation in MATLAB. This project included of 3 phases which are hardware setup, system modelling and validation, and also classic synchronous controller. Synchronous control of twin axes drive table project focused on obtaining a modelling transfer function and design by simulation of a classic PID controller that approach zero synchronous error for its performance.

ABSTRAK

Dual paksi meja sistem merupakan aplikasi yang selalu digunakan dalam industri. Kawalan segerakan digunakan untuk pemanduan yang cekap pada meja pemacu paksi kembar yang secara serentak didorong oleh dua motor linear DC yang dipisahkan. Penjejakan ralat kedudukan ialah parameter yang paling penting untuk diperhatikan dalam meja pemacu kembar. Pada halaju yang tinggi, meja pemacu paksi kembar perlu mendapatkan kesilapan sifar dalam kedudukan untuk kedua-dua paksi. Selain itu, penyegerakan pada meja pemacu paksi kembar yang disambungkan secara mekanikal menjadi cabaran utama. Hal ini demikian, kerosakan akan berlaku apabila penyegerakan gagal. Projek ini bertujuan untuk mendapatkan dan mengesahkan matematik fungsi pemindahan pemodelan yang tepat dengan eksperimen. Ketepatan pada matematik fungsi pemindahan pemodelan ini adalah amat penting kerana ia akan mempengaruhi banyak dalam proses mereka pengawal selanjutnya. Selain itu, projek ini juga bertujuan untuk merancang pengawal segerak yang menghampiri kesilapan sifar dengan menggunakan simulasi dalam MATLAB. Projek ini termasuk 3 fasa iaitu persediaan perkakasan, pemodelan sistem dan pengesahan dan juga rekaan pengawal segerak.

TABLE OF CONTENTS

LIST OF TABLES

LIST OF FIGURES

CHAPTER 1

INTRODUCTION

1.1 Overview

Generally, synchronous control on twin axes table drive which configured parallelly has been designed and developed in various projects by using different driving mechanism either with the ball-screw driven system or the direct drive driven system. This chapter will discuss few sub-topics on motivation, problem statement, objective, scope and organization of report.

1.2 Motivation

During this new era, automation is the most important sector developed for the industrial sector. Dual axis ball-screw driven table is widely used in industrial application such as large gantry type machine tools and positioning stages [1]. For the industrial application, the table is coupled on two axis linear guide apart for a long span. For this configuration, synchronization is done to prevent danger and damages that will occur on the system. Synchronous control needed in the dual axis driven table had been applied in various industries such as printing, plastic, textile, rubber, iron and steel [2] which involved large gantry type machine tools. Besides, synchronous control system is applied in automatic field which used to control dual axis brushless direct current motor used in

the electric vehicle. For fast and precise motion, synchronous control is important for the dual axis drive table.

Synchronous control is a method that used for any simultaneously moving hardware as it provide additional corrective action in synchronous performance. In a synchronous control system, zero synchronization error is the optimal requirement. To obtain approximate zero synchronization error, position tracking error is measured and eliminated by a simple algorithm that calculate an error of the difference between reference position and actual position. There are several existing synchronous control methods such as synchronized master command generator control, conventional master-slave motion control, cross-coupled motion control etc.

Ball screw technology is commonly used since industrial era as direct drive system facing challenges in control strategy and materials at early 18's when Wheatstone proposed and developed the first direct drive system. Due to the technology of control system and materials nowadays, development of direct drive system had more application and development. For the requirements of high acceleration and high precision drive system, advantages of direct drive system become more significant while compared with ball screw system [3]. The technical advantages of direct drive system are it provide a gearless system that helps to reduce friction, to eliminate backlashes and is high mechanical stiffness [4]. However, the disturbances occurred from the inertia and forces variations which caused the direct drive system tends to be slow. Besides, direct drive system is easily affected by the problem of magnetic isolation and protection [3]. Comparing with direct drive system, ball-screw driven system is Due to the affordability and resources, a dual-axes ball screw mechanism is decided to be used in this project. Before developing the control system, a modelling of the dual axis drive table is developed by kinematic mathematically wise.

1.3 Problem Statement

The twin axes drive table that driven by the direct drive system that parallel coupled with each other by a table or called stage facing some challenges such as damages caused by synchronization failed and hard to approach the ideal situation of precise synchronization. To prevent the dangers and damages, synchronous control design on the motion of both linear guide motor that mechanically coupled in twin axes table drive becomes the main challenge of the twin axes table drive system. Besides, a most precise synchronous control system that approaches zero synchronous errors at relatively high velocity is also one of the challenge needed to be overcome.

1.4 Objective

Synchronous control on twin axes table drive is aimed;

1. To construct and obtain the parameters of the model of dual axes table driven by ball screw.
2. To obtain the kinematical mathematical model and validate the accuracy of modelling in simulation and experiment.
3. To propose a classic controller design for closed-loop performances evaluation.

1.5 Scope

In the synchronous control on twin axes table drive, the hardware configuration included 30V direct current motors, ball-screw mechanism, linear guides, linear encoders, power amplifier, and accelerometer which produce a twin axes table drive that travel about 200mm with maximum 5m/s. Besides, the table (stage) can afford load at maximum of 20kg during travelling. In this paper, kinematical mathematical wise modelling will be focused more and the synchronous controller design by cross coupled control method will be developed.

1.6 Organization of Report

In this report, it will be written in five chapters which are introduction, literature review, methodology, expected result and conclusion.

Chapter 1 is mainly describing the project outline with the motivation which supported by facts and background of the project, necessary elements covered in problem statement, objectives of this project, and the scope of the project which described the project configuration and works included for it.

Moreover, the project historical background and the theory which related to this project is described and explained in Chapter 2, literature review. In this chapter, the factors of mechanical and electrical components are discussed that affecting the Twin-Axes Table Drive System with the mechanical design and electrical design. It discussed about the comparison between previous projects.

For Chapter 3, methodology shows the hardware design in mechanical and electronic design and offerings the assembly of twin-axes table drive system chosen that were developed.

In Chapter 4, all results will be presented in graphical form and table form with the detailed discussion for the results. The mathematical modelling of twin-axes table drive system is obtained through MATLAB. The synchronous control design is done in simulation environment of Simulink. The simulated controllers will be tested on real plant for performance evaluation.

Lastly, Chapter 5 will provide the summary of this project and the future work that be suggested for improvement purposes.

1.7 Summary

This chapter concludes the importance of synchronous control on the twin axes table drive system. It summarized the limitations of the synchronous motion which the load weight becomes the direct disturbances onto the two axes ball screw mechanism. Besides, the main requirement of position tracking accuracy issue due to both axes driving by separated motor and unbalanced disturbances acting on it. The key to this enabling technology is the development of an optimal synchronous controller and optimum sensing platform which are highly reliable, robust and accurate.

CHAPTER 2

LITERATURE REVIEW

2.1 Introduction

In chapter 2 literature review, project background and the theory that required during the course in previous study related to synchronous control on twin axes table drive system is presented.

In the first section of this chapter, an overview on the project and its history background will be discussed. Next, it deals with the theory and working principle of Twin-axes Table Drive System. Then, the mechanical design for the twin-axes table drive system and the previous works of modelling and synchronous motion control method will be discussed. Lastly, the summary of literature review is written.

2.2 Overview of Twin-Axes Table Drive System

Twin-axes stage application is invented since late 1980s. A twin-axes stage is defined as a mechanism that mechanically coupled of two parallelly arranged linear axes by a stage or a table with a specific span that defined based on the application. This mechanism helps to reduce the potential skewed cause by the unbalanced loads applied on the table comparing to the single axis table drive system [1]. In existing real-world application, the twin axes table drive system is widely used in industry large gantry type machine tools such as large working range CNC mill machine etc.

There are different motors, direct drive motor and ball-screw driven by direct current servo motor are used in previous similar researches. Both motors are suitable for this application according to the requirements and the improvement of technology during this new era. From the previous researches by Yunjun Chen [9], an intelligent control with feed-forward control method is studied and designed for the two-axis strict dynamic synchronous process which moves on a rotating shaft that driven by a servo motor. Moreover, Jung-Hwan Byun and Myung-Soo Choi [10] had also studied on the method for modelling and control of a dual parallel motion stages that driven by a servo motor that coupled with a lead screw system. Other than that, Min-Fu Hsieh [1] has studied on the synchronous control scheme and system modelling technique of a single-axis stage that dual axis ball screws system. Hsieh studied the modelling and control scheme with the method of cross-coupled control algorithm.

Yasufumi Yoshiura and Yasuhiko Kaku [11] have carried a research on the synchronous control apparatus that able to synchronously control the motion of plurality of motors with the usage of linear motor/ direct drive motor. In the synchronous control apparatus study, Yasafumi and Yasuhiko used a prototype of one coupler connecting two parallelly arranged axes of motors.

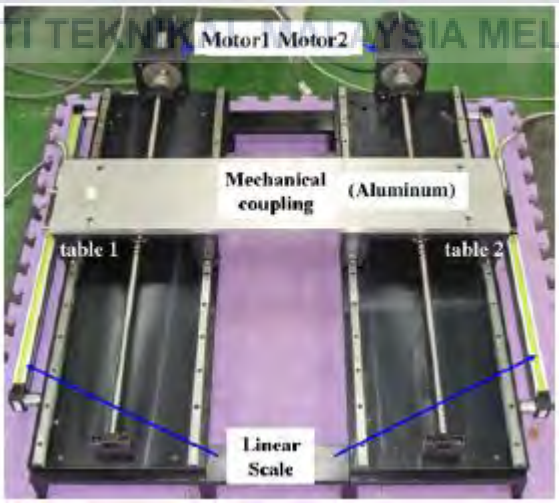

Figure 2.1 Configuration of single axis stage driven by dual axis ball screws system [1]

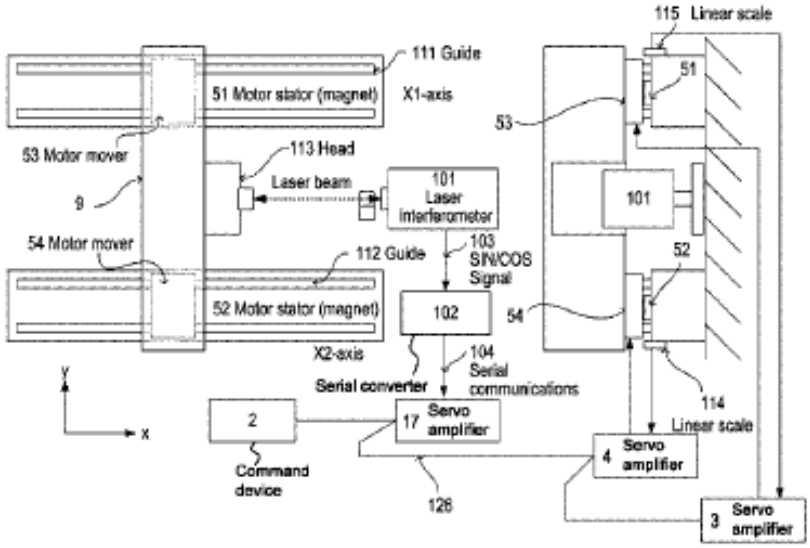

Figure 2.2: Drawing of the dual axis table drive [11]

The main focus in this project is to has the most accurate modelling transfer function and to design a synchronous controller on the Twin-Axes Table Drive System.

2.3 Twin Axes Table Drive System

The dual axes driven stage application has been using in industrial motion control apparatus such as machine tools and positioning stages since late 1980's. Twin axes table drive system is a mechanism that configured to drive single mover or table that act as the coupler between two parallelly arranged linear axes that driven by any type of motor.

From previous research by Min-Fu Hsieh [1], the dual ball-screw stages in machine tools are capable to be precise in motion. However, the precision in a large ball-screw driven stages decreased as the span across both linear guide increased. Min-Fu Hsieh [1] and Baeksuk Chu [12] have studied on the synchronous control of dual drive system where the system is driven by large ball screw mechanism that drive the moving beam with identical actuators.

Other than that, Mi-Ching Tsai, Min-Fu Hsieh and Wu-Sung Yao [13] have studied on the synchronous control of dual axes stages that the moving beam driven by linear motors despite of using ball screw system to drive the stages in order to get high-speed and high-accuracy performances.

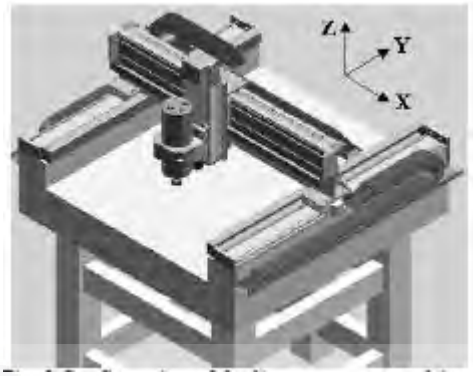

Figure 2.3: Configuration of linear servomotor driven machine tool [13]

As shown in Figure 2.3, linear motor, the gearless driving system with its non-contacting energy translation and high acceleration essences, have been increasingly applied in high-speed and high-accuracy industries [13]. However, its control of the servo is more difficult due to the sensitivity of linear motor that the load weight changing on the mover that coupler on it will be the direct disturbances for linear motor [3]. Hence, it can be concluded that ball screw still plays an important role in multi-axis stage application as it precise positioning performance and its capability in long range for positioning, travelling and contouring actions [14].

2.4 Working Principle of Twin Axes Table Drive System

In this section, the working principle of twin axes table that drive by linear motor and ball screw mechanism will be discussed. The advantages and disadvantages of both actuators will be discussed in each part for the comparison purpose.

2.4.1 Twin Axes Table Drive by Linear Motor

A linear motor has a similar principle with DC servo motor where a linear motor can be illustrated as a split and stretched rotary DC servo motor as shown in Figure 2.4. Both rotary motor and linear motor works on the Lorentz' Laws where the force (F) is induced when the current (I) along the vector distance (L) and the flux density (B) interacted. The following equation shows the relationship of the parameters occurs on the linear motor.

$$\vec{F} = I\vec{L} \times \vec{B} \tag{2.1}$$

As the induced force result onto the wire (current carrying media), motion is produced based on the Fleming's Left-Hand Rule.

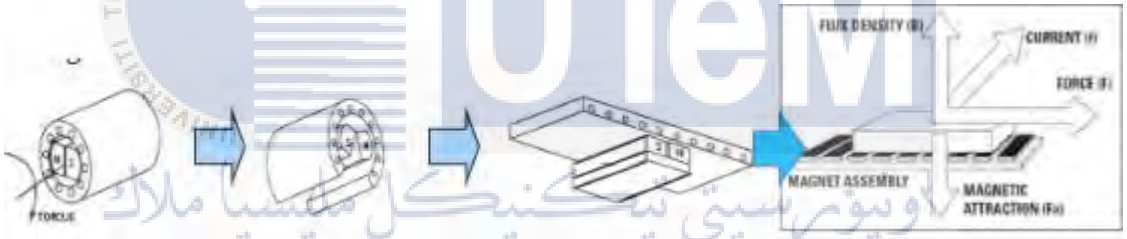

Figure 2.4: Illustration of structural evolution of a rotary motor to a linear motor [17]

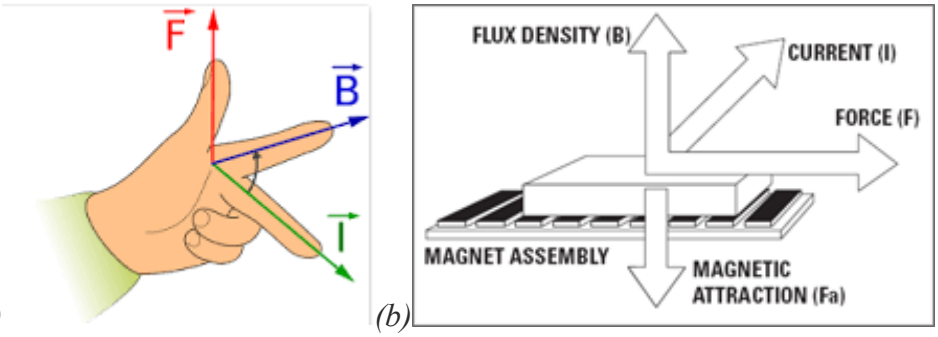

(a) *(b)*

Figure 2.5: Visualization of (a) Fleming's Left- Hand Rule Determination [18] and; (b) Direction of force produced as the direction of the motion [17]

The differences of the linear motors with rotary motors are the stator in the rotary motor is replaced with a forcer at the same function while the rotor of the rotary motor is now becoming a coil and magnet rail that works for same function.

Followed by the advancing technology nowadays, usage of linear motor gradually increased as it provides high speeds, high precision fast response, higher stiffness, zero backlash and maintenance free operation. However, pros and cons come together, the linear motor needed higher bandwidth to drives and controls, has higher thermal heating caused by the load attached to the mover or forcer which increase the resistance on the forcer and lead to higher power losses ($P = I^2R$). The most significant downside of a linear motor is it is expensive when comparing with other types of motors [15].

2.4.2 Twin Axes Table Drive by Ball Screw Mechanism

From Figure 2.6 and Figure 2.7, it shows the same working principle of linear motor in working principle of DC rotary motor. However, in DC rotary motor, the electrical current (i) passes through a coil in a magnetic field (B) produced by the stator, and the magnetic force produces a torque (T) which turns the DC motor based on Right-Hand Rule shown in Figure 2.8. The working relationship of a DC rotary motor can be illustrated by the following (2.2).

$$T = K_t I \tag{2.2}$$

where the K_t is the torque constant in newton-meter per ampere.

The DC rotary motors are widely used since late 1980's. It is now still using in industrial field as it is cheap, simple to be constructed and easy to be controlled as the speed is governed by the voltage and torque by the current through the armature. However, the DC rotary motor produces noises and has shorter life cycle as there are friction produced whenever the rotor turning with the mechanical brushes.

The DC servo motor is chosen as the actuator for Twin Axes Table Drive System as it is cheaper and easier to obtained from market. Moreover, the DC servo motor has easier design and construction path by coupling with a ball screw after comparing to the linear motor since this project focused more on the synchronous control of the system rather than the motor performances in the system.

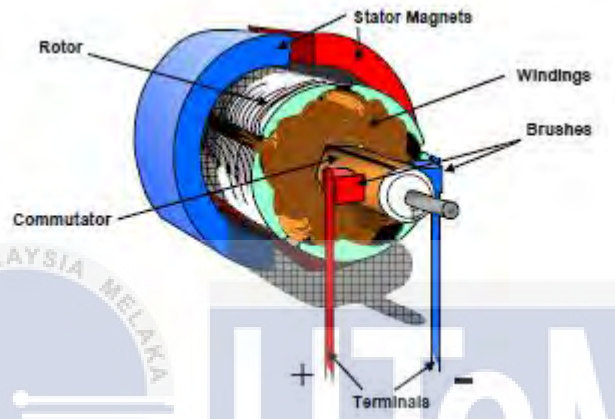

Figure 2.6: Construction of the DC rotary motor [16]

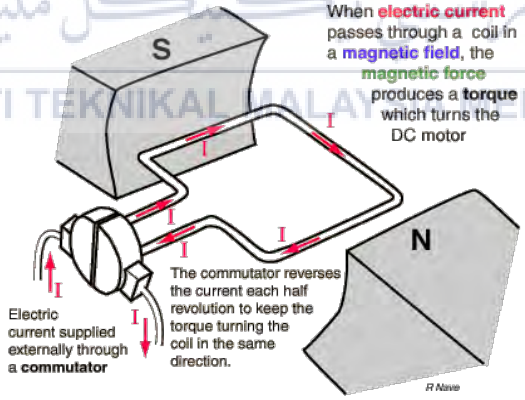

Figure 2.7: Visualization of the movement of the coil during current flows [17]

2.5 Mathematical Modelling

Mathematical models are critical to understanding and accurately predicting the behavior of complex systems where it can complete the following tasks such as forecasting and optimizing system behavior, designing control systems and characterizing system response [19]. Mathematical modelling is used in varied types of system which are, linear and nonlinear system, static and dynamic system, deterministic and stochastic system, and also discrete and continuous system [19]. In a model, system dynamic equation is developed from the system free body diagram (FBD) that the set of forces and moments which represent the action at that connection [20].

Jia En Foo et al. has concluded that a ball screw mechanism inhibits nonlinear behaviours in micro movement that affects the performances [14]. The nonlinear behaviours of ball screw mechanism is caused by hysteresis, Stribeck effect and nonlinear frictions of the screw shaft. In [21], Xiang, Qiu and Li modeled the non-linear frictions in the ball screw mechanism with LuGre friction model. Jia En Foo et al. [14] has constructed the mathematical modelling that describing the macrodynamics as the setup is shown in Figure 2.8.

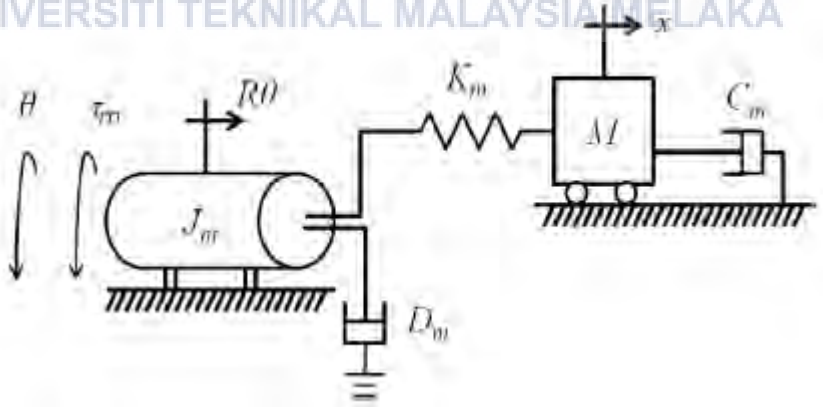

Figure 2.8: Free body diagram of ball screw mechanism [14]

In [1], Min et al. constructed the modelling of single axis ball screw mechanism that focused on the thrust to drive the slide table with neglected the friction effect of the ball screw. This model is constructed from the free body diagram illustrated as shown in Figure 2.9. However, Min et al. did take in consideration of mutual influence caused by the coupling effect of the sliding table. In [10], Jung et al. has modeled the ball screw mechanism by taking the driving factor of servo motor into consideration as shown in Figure 2.10.

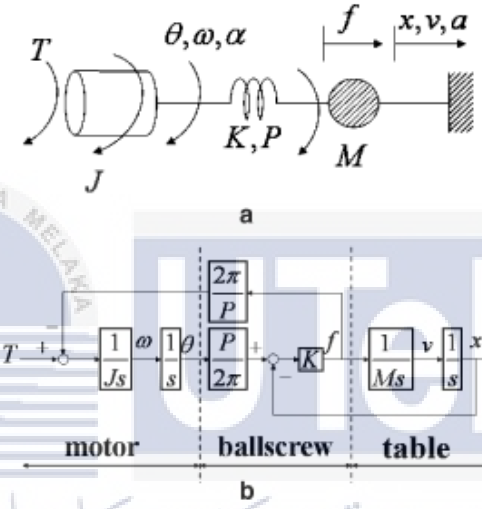

Figure 2.9: Single-axis ball screw angle (a) The model; (b) The block diagram [1]

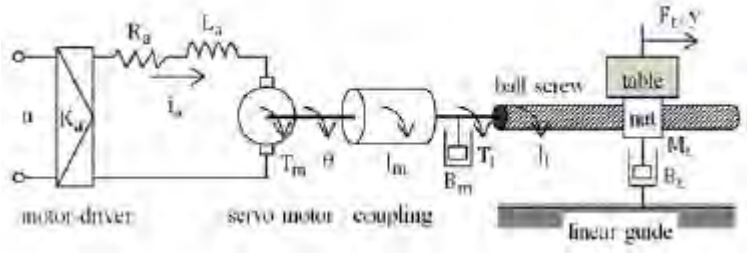

Figure 2.10: Free body diagram of the single axis motion stage [10]

In conclusion, a free body diagram is constructed with consideration of the set of forces and moments that occurred in the system. The free body diagram will be then used in the modelling.

For a mechanism modelling, there are several methods to achieve the modelling transfer function result. In [11], Yasafumi and Yasuhiko used conventional lumped modelling method for the complete modelling for the synchronous system. In [26], Viktor et.al proposed and discussed on the lumped model method for the parameters value extraction and unlumped model method for the comparison of accuracy of the value. They compared the transient performances of the system and used the conventional lumped model method which used the load cells and compared the results for coefficient value.

In [25], Chou et.al. described that LuGre Friction modelling method did accurately on complex static and dynamic characteristics such as stick-slip, presliding displacement, viscous frictions, Coulombs frictions and Stribeck effect occurs on the dual axes table drive. LuGre friction model described the mechanism in detail. However, this increased the order modelling or macrodynamic modelling.

In [27], Liu et.al. explained the Dahl Model that assumed the ball-bearing friction as the solid friction which does not included the Stribeck effect and stick-slip motion that have been considered in LuGre friction model. However, Dahl model has the simplest model as it is a first order dynamic system.

Lastly, Karl and Carlos introduced Hybrid mathematical modelling that took position output by the mover and the thrust output from the actuators in the system in [28]. Karl and Carlos found that the parallel control or called as cross-coupled control model appears to produce better performance than the hybrid control model did.

From the literature did, the lumped modelling method success to lump the system parameters together and able to reduce the order modelling or macrodynamic modelling while compared to the other modelling methods. As the simpler design of this approach, mismatch and parameter variations becomes the most concerned unwanted disturbances to be removed for higher precision.

2.5.1 Parameters measurements

To obtain the unknown parameters such as viscous friction coefficient etc. in the model, the load cell is used for the friction measurement. As we known that friction force is the product of normal force and friction coefficient.

$$F_f = \mu N \tag{2.3}$$

where

F_f = Total frictional force (N)

M = Friction coefficient

N = Normal force (N) = mass x gravitational force (9.81N)

The load cell will be placed at the position that mated of 2 connected surfaces. In this case, the motor viscous friction and the viscous friction applied by the mass are needed to be measured by the load cell during the movement of ball screw [34] [35]. Other than that, the motor inertia (kgm^2), rotational stiffness of screw shaft (N/m), mass of table (kg) will be measured or weighed directly with weighing instruments.

2.6 Synchronous Motion Control

Different control methods and different controller design will be discussed in this part. Synchronous control is a control method that control simultaneously motion of multi-axes drives that provide additional corrective action in synchronous performances. In a dual axes mechanism, position tracking error will be the focused error in synchronous motion.

2.6.1 Control methods

Several control methods are used for synchronous motion control for a system. In [22], Lorenz and Schmidt had classified the synchronous control techniques into three categories, which are synchronized master command generator control, conventional master-slave motion control, and relative dynamic stiffness motion control. For jointed axes with two motors, Hsieh, Yao and Chiang [1] have studied on the cross-coupled control which the compensation is made by considering of the mutual influences created by the table between 2 tables. From Hsieh, Yao and Chiang [1] research, the cross-coupled control method is concluded after comparison with the other two control method.

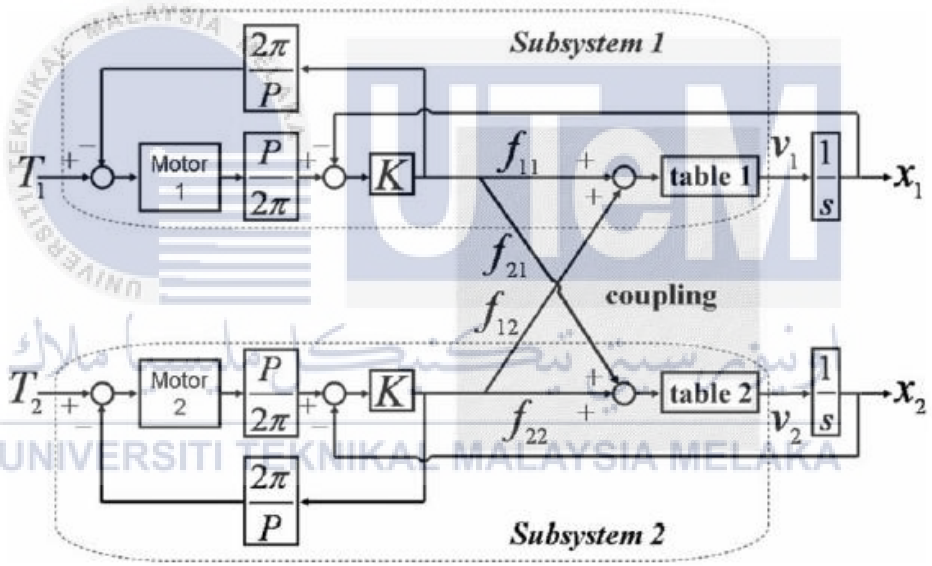

Figure 2.11: Block diagram of the coupled system [1]

A synchronized master command generator control sends same commands to both motors in an individual control loops. In [23], Huang et.al. have focused on the development of error modelling using the synchronized master command generator control in neural network. The control modelling of dual axis stage is shown in Figure 2.12. However, this control method has the least accuracy for synchronizing motion as the compensation and command is sent separately to the driving motor.

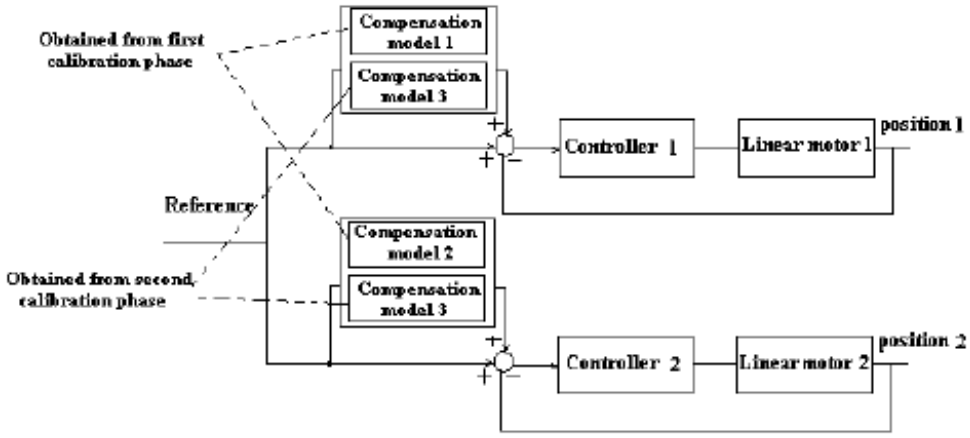

Figure 2.12: Synchronized master command generator control with compensation for dual axis stage [23]

In [13], Hsieh et al. had modeled a synchronous control scheme using master-slave control method that position control is applied to one motor in one of the axis, while velocity control is applied on the slave motor. Position is detected by the slave system by the velocity/ positional ratio, $\frac{dx}{dt}$. The relationship of the master control system and the slave control system is shown in Figure 2.13.

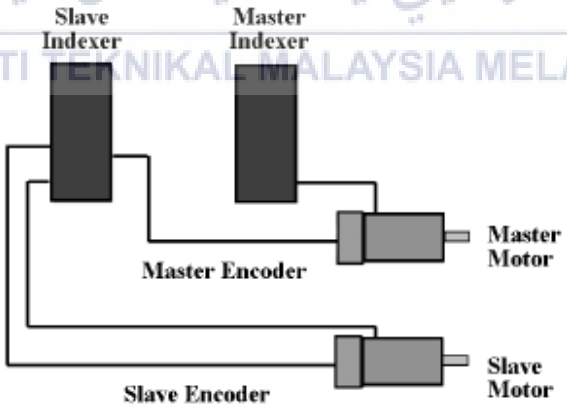

Figure 2.13: The configuration of master-slave control system

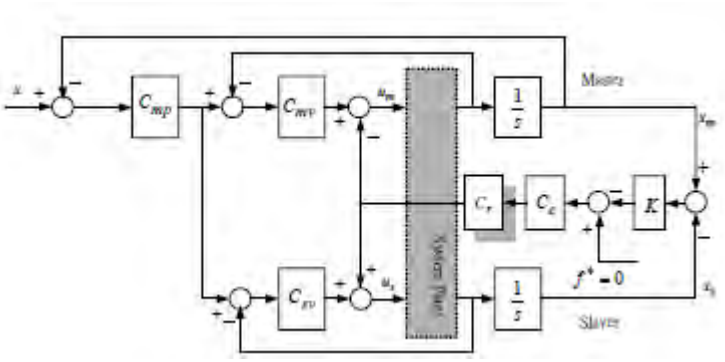

Figure 2.14: Synchronous control modelling by master-slave control

In [2], Chen, Jiang and Yang had developed an intelligent control system by using master-slave control method in combination of intelligent variable parameter control and intelligent feed forward control.

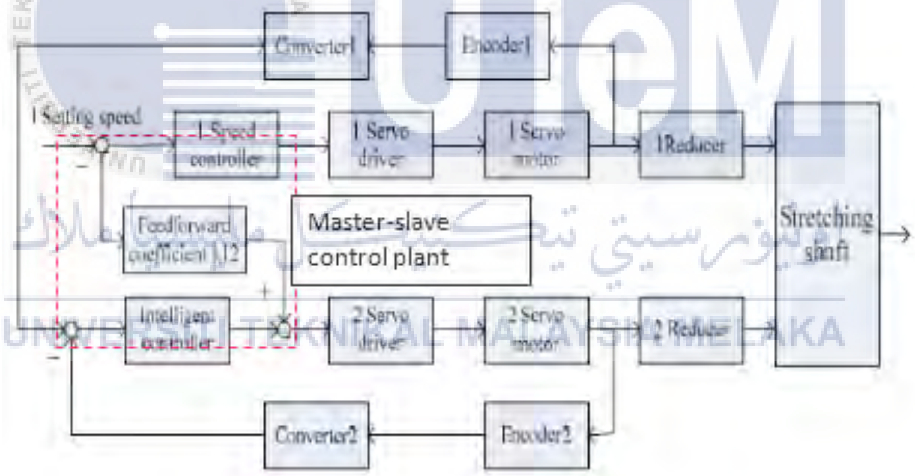

Figure 2.15: The synchronous control block with master-slave control method [2]

In this project, master-slave control method and cross-coupled control method will be modeled and tested for the synchronous control of the system and its performances tests. This is due to the accuracy of these two control methods will be higher compared to the synchronizing master command control method.

2.6.2 Controller Design

The basic controller design used in current industry is Proportional Integration Derivative (PID) controller. In [24], Yuxin Su, Dong Sun, Lu Ren and James studied on the integraed control which consist of PI and PD synchronous control method for a high-precision motion of parallel manipulators. In their claim, the saturates PID control gave rise to global asymptotic stability for a local PID feedback. In [12], Chu, Kim, Hong, H.K. Park and J.Park has used propotional control algorithm with the synchronizing control add on to provide additional corrective action for specially improving the synchronizing performances. They had concluded that the propotional controller is a conventional technique in independent axis control.

In [2], Chen, Jiang and Yang used the combination of intelligent feed forward control and intelligent variable control for speed and displacement controller that reached the error ration of 0.5 in it research. They claimed that synchronization of two axes can not be achieved by conventional algorithm.

However, Chou, Lin, Chen and Lee studied on the sliding mode control (SMC) for the synchronous control as it is insensitive to parameter variations and external disturbances on the sliding system. Moreover, the SMC control helps in development of on-line learning algorithm. [25]

In conclusion, a conventional proportional controller for this project as to ensure the performances of the closed-loop characteristics for this system. Due to the complexity of SMC controller and combination of control in [2], it is not proposed for this project.

CHAPTER 3

METHODOLOGY

3.1 Introduction

The project is divided into three phases to achieve all objectives which shown in Figure 3.1. There are 3 main phases which briefly described the working flow to achieve each objective.

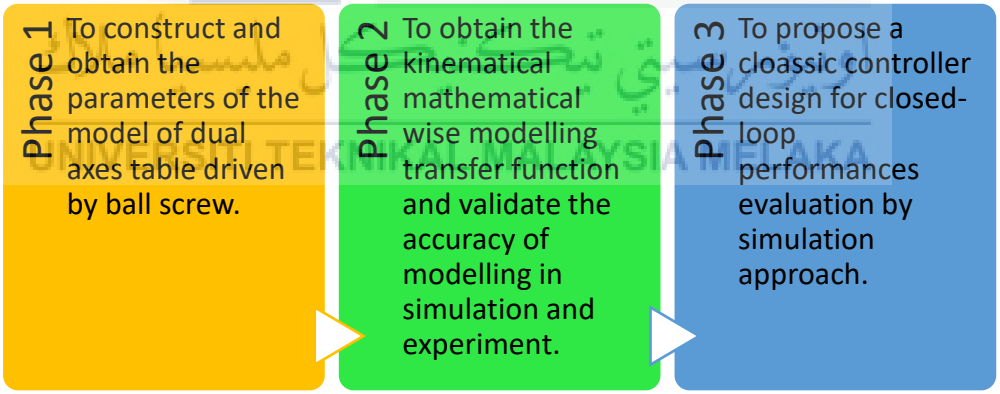

Figure 3.1: Phases of project to achieve each objective

In this chapter, the designed system of hardware and software will be discussed in detail in term of mechanical hardware selection, experiments that designed to evaluate the performance of the designed system and the control method that used for synchronous controller.

The project flow chart is listed out the overall process that has been taken for the project completion. Figure 3.2 shows the brief idea about the flow of project from planning, information gathers, design, until fabrication and experimental test. The steps taken are further explained in next section.

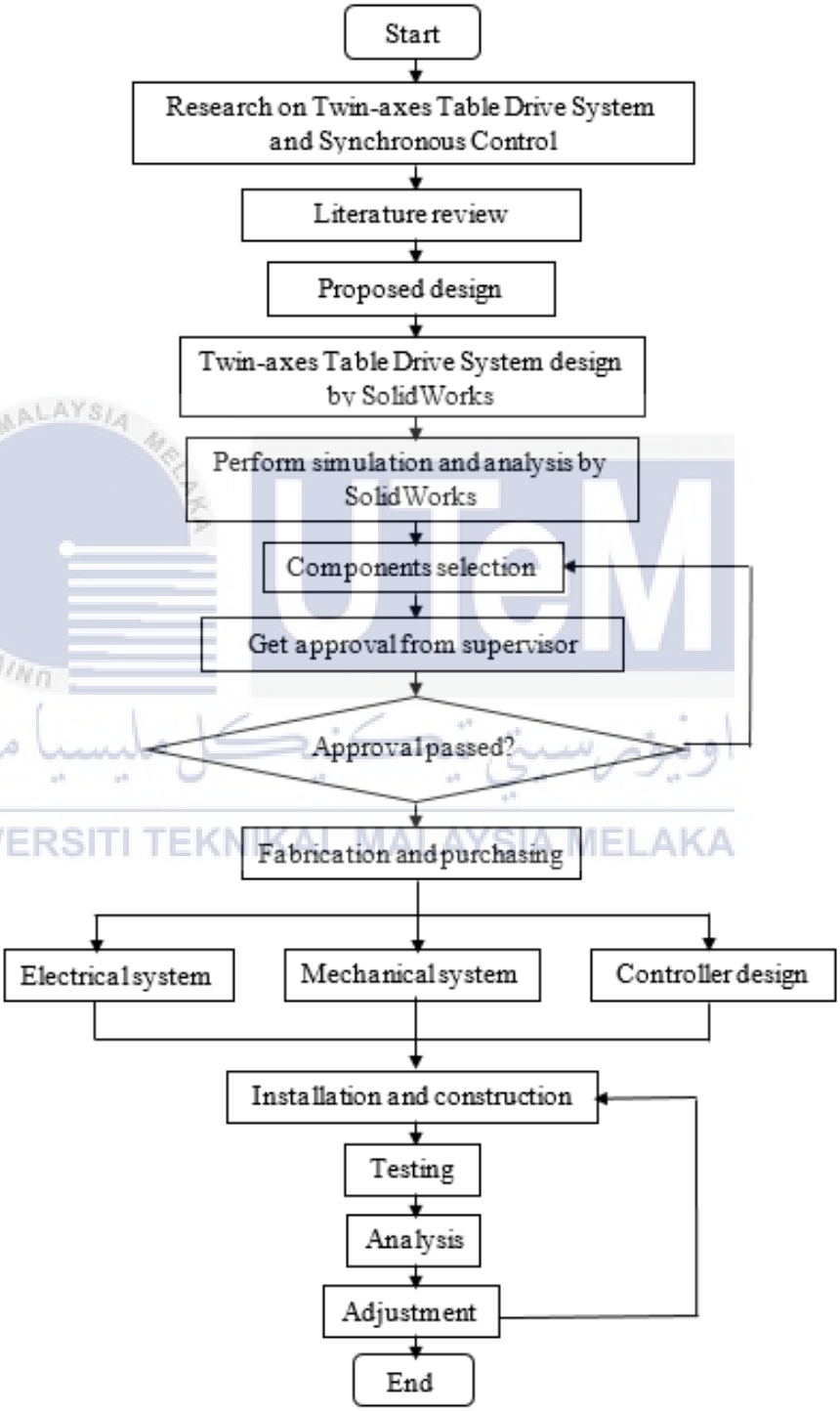

Figure 3.2: Project flow for twin-axes table drive system

3.2 Working Methodology During Phase 1

To achieve first objective, hardware construction of a twin axes table driven by ball-screw system is set up. To complete the hardware setup, researches are done, and the components needed are listed. The components needed in the hardware setup are as listed, 2 direct current servo motors, 2 ball screw systems, 2 linear encoders, 2 linear guides, one basement, and a coupling table. Based on the previous ball screw project done by Jia En Foo [14], the model of DC servo motor, linear encoder, ball screw shaft and the linear guide are confirmed. The components are resourced or bought based on the compatibility for each other and the basic requirement to have a minimum 200 mm range of travelling.

Next, resourcing is done to find the most suitable components with satisfied specification from internet distributors or manufacturers for the rest from the components list. Then, comparison between different manufacturers for the same item to be purchased is done to select and decide the most suitable component in term of specification and cost. To visualize the hardware configuration of the system, the design of the hardware is drawn with SolidWorks. Lastly in this phase, the system is setup according to the design drawn and approved and calibration has been done before experiments started.

3.2.1 Twin-axes Table Drive System Basement and Mover

The Twin-axes Table Drive System needed a foundation that support and fix the construction of the Twin-axes Table Drive System components. All the components used in the configuration of twin-axes table drive system will be fixed on the basement that shown in Figure 3.3 below. The basement is a tooling base that needed for the installation of ball-screw, linear guides and the direct current motors. The basement chosen as in Figure 3.3 is with the dimension of 350 mm x 250 mm.

Figure 3.3: Basement for twin-axes table drive system

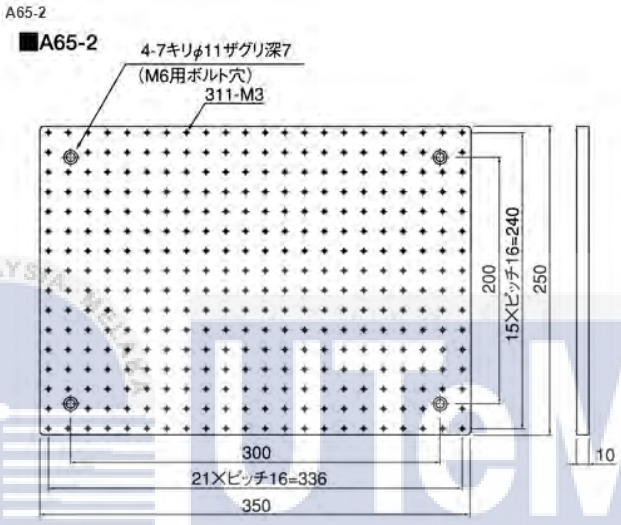

Figure 3.4: Detailed 2D CAD drawing of basement

Figure 3.4 shows the details of the basement which labelled with the screw holes dimension and the base dimension. As the reasons stated in other section, this basement is chosen to be used in this project.

Moreover, the mover plays an important role to carry loads. The diagram of mover is illustrated in Figure 3.5. In the twin-axes table drive system, both ball screw axes are separated with a span of 50mm.

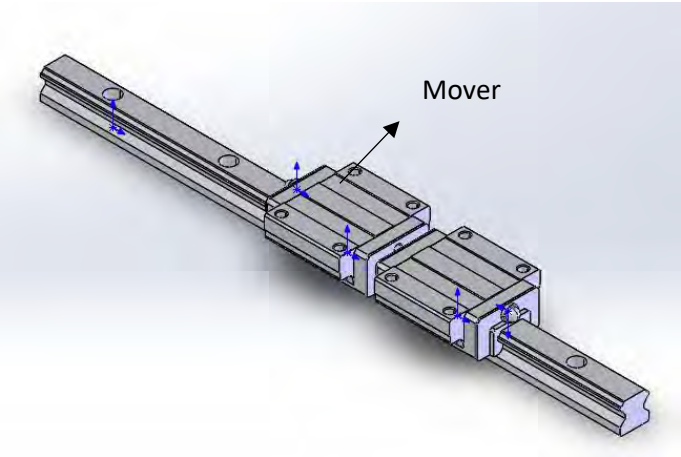

Figure 3.5: Mover of the twin-axes table drive

3.2.2 Linear Guide

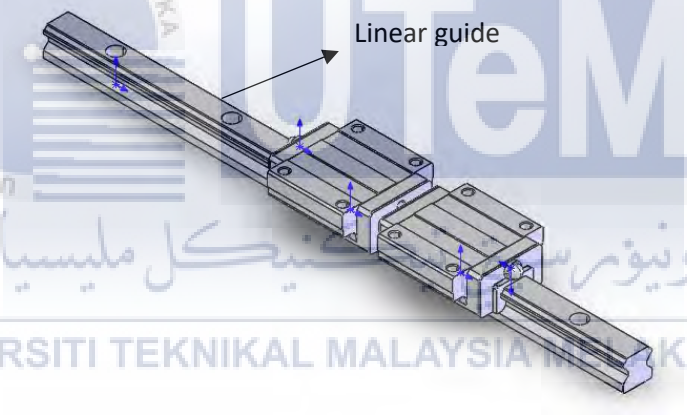

Figure 3.6: Linear guide of the twin-axes table drive

Linear guide is used as a guideline for the motion of the mover which coupled on the lead screw that driven by the direct current motor. The linear guide is operating with ball bearings run at each side of the mover to ensure the straight and stable motion of the mover driven on the lead screw.

3.2.3 Linear motion actuator – Direct current motor

Generally, the linear motion of the ball screw system is generated by an actuator. In twin-axes table drive system, the ball screw axis system needed a rotary motor to be driven. Rotary motors are capable to generate rotary motion either in clockwise or counter clockwise. Hence, the ball screw can be driven by the rotary motion generated. A ball screw mechanism is working on the principle that translation from rotary motion into linear motion that perform by the mover.

Advantage of using direct current servo motor is due to the ease in speed and positioning control that makes the direct current servo motor as the preferable option other than linear motor. Direct current servo motor RS-263-6011 manufactured by RS-Pro is used in twin axes table drive system as sufficient torque needed to carry load of 10kg as shown in Figure 3.7. The specification of the direct current servo motor RS-263-6011 is listed as in Table 3.1.

Figure 3.7: Direct Current Servo Motor RS-263-6011

Table 3. 1: Table of specifications of rotary motor RS-263-6011

Parameters	Value
Maximum output torque (Ncm)	36
Supply voltage (V_{dc})	24 – 30
Output speed (rpm)	1600
Power rating (W)	30
Stall torque (Ncm)	12
Shaft diameter (mm)	6
Length (mm)	88
Width (mm)	66
Dimensions (mm)	66(Dia.) x 88
Rotor inertia (kg.cm^2)	0.214
Current rating (A)	1.3

The rotary motor is coupled with ball screw mechanism. The ball screw acts as the translator from rotational motion to linear motion that performed by the mover (or dummy loads).

Figure 3.8: Lead screw components

The lead screw used in the twin axes table drive system as shown in Figure 3.8 is with diameter of 8 mm per revolution and length of 320mm. The rotary motor is coupled with the lead screw by the cylindrical coupling that with dimension of 18.05 mm (Diameter) x 25.24 mm (Height). The coupling diagram is shown in Figure 3.9.

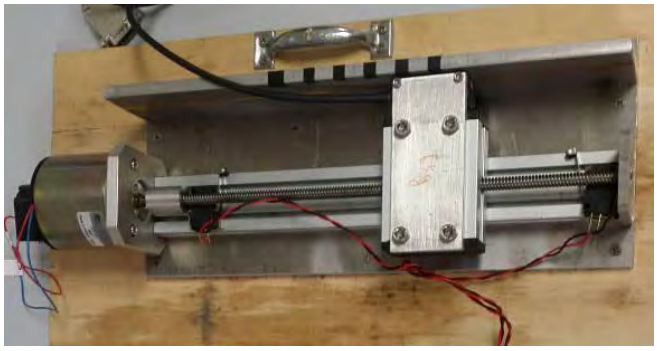

Figure 3.9: The coupling diagram of rotary motor and lead screw

3.2.4 Design and Construction of Twin Axes Table Drive System

According to the dimension of all resourced or purchased components, the working hardware configuration is drawn with SolidWorks with all mechanism parts assembled as shown in Figure 3.10. According to Figure 3.10, the hardware has been set up and is modified to get smoother operation for further experiments.

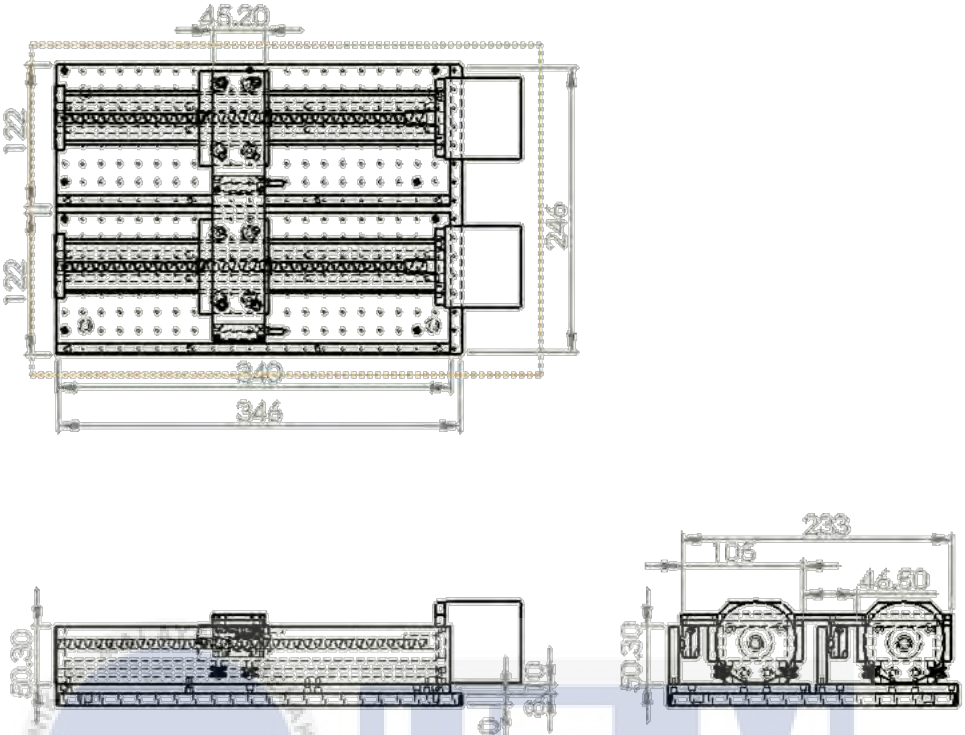

Figure 3.10: The 2D layout view of the Twin Axes Table Drive System.

3.3 Working Methodology During Phase 2

To achieve the second objective, a system modelling transfer function is developed on kinematical mathematical wise. A system block diagram is drawn based on the actual ball screw system for single axes and dual axes to show the interfaces between each component in the system. Next, the free body diagram is drawn and labelled based on the actual single ball screw system that showing the model parameters such as frictions that will occur on the system during movement, forces that will be applied or generated on the system and other disturbances. According to the system block diagram and the free body diagram of the system, a transfer function is generated for single axes ball screw. To extract the unknown variables of the system, lumped modelling method with the usage of load cell has been done for both axes system.

After the parameters obtained, transfer function of the dual axes table drive system has been generated. This modelling transfer function will next to be tested by simulation in MATLAB. Then, experiments of open-loop and closed-loop transfer function will be conducted on the actual twin axes ball screw drive system separately for single axis driven and twin axes driven. The experimental data collected will then be analyzed and compared with the simulation results to achieve the second objective.

3.3.1 Voltage Amplifier, Power Amplifier

The 30V direct current servo motor, RS-263-6011 used in this project needed minimum 24V supply voltage with 1.3A rated current for its driving purpose. This direct current supply needed to be generated by a voltage amplifier that output the relative voltage and current. In Figure 3.11, the 24V power supply is needed as the driver for both direct current motors.

Figure 3. 11: 24V power supply with output 1.8A

3.3.2 Linear Encoder

An encoder is a sensor, transducer or reader head that used to read the measurement on the system which may convert the reading into an analog or digital signal. In the twin-axes table drive system, a linear encoder act as a sensor readhead that read the

encoder position on the paired linear scale. The encoded position read by the linear encoder will be convert from analog reading into digital signal.

In this project, Renishaw RGH22A30L00A and RGH22D30L00A are chosen as the linear encoder for the position recognition. This readhead is the main part of the encoder and the linear scale is needed for the position reading purpose. This type of linear encoder has an analogue output signal with 1 V_{pp} differential, equipped with the incremental type. Figure 3.12 shows the RGH22A readhead and Figure 3.14 shows the specification of the linear encoder. Figure 3.13 shows the type of connector that uses for the linear encoder to connect to the data acquisition devices while Table 3.2 listed the port function of all of the used ports.

Figure 3.12: Readhead and linear scale of RGH22A

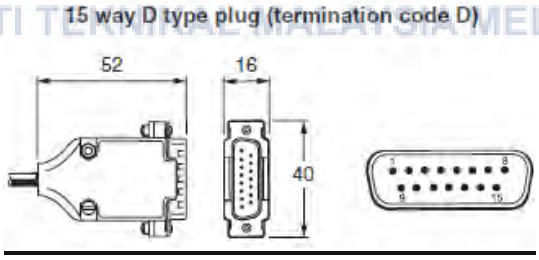

Figure 3.13: The connector view of the RGH22A

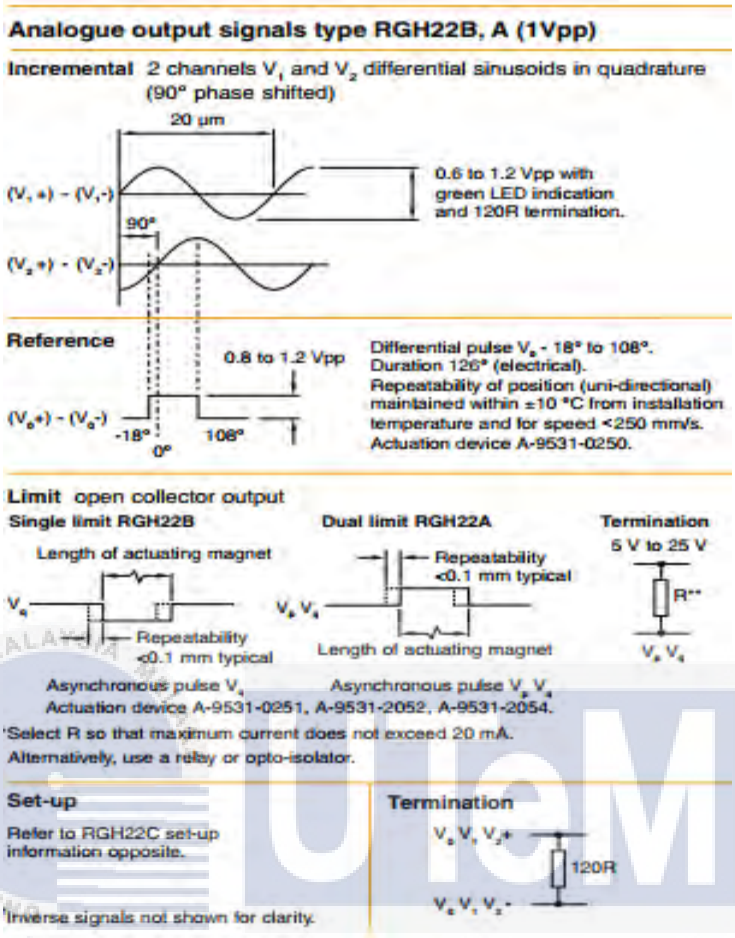

Figure 3. 14: Specifications of RGH22A readhead

Table 3.2: Port function of Linear Encoder Connector

Linear Encoder	Function	Port Number
RGH22D30L00A	5V	7
	0V	2
	A+	14
	B+	13
RGH22A30L00A	5V	4
	0V	12
	V_1+	9
	V_2+	10

3.3.3 Data Acquisition (DAQ) Device – MICRO-BOX

Data acquisition is the process of measuring an electrical or physical variable such as voltage, current, temperature, pressure or sound with a computer [5]. A DAQ device is a device that acquires data samples [6] by communicating the central control and the recording system with a cable or radio waves [7].

Figure 3.15: Block diagram of a measuring system [5]

Figure 3.15 is the block diagram that shows the interfaces between sensor, DAQ device and computer along the measuring system. It can be seen that DAQ device is the most important device that digitizes incoming analog signals that ease the process of interpretation by the computer [5]. To complete the measuring system, DAQ device is completed with 3 main parts which are signal conditioning circuitry, analog-to-digital converter (ADC) and a computer bus. However, some of the DAQ device did included digital-to-analog converter (DAC) for output analog signals into the plant system.

In this project, linear encoder used in twin axes table drive system is interfacing with the computer through Micro-Box 2000/2000c as shown in Figure 3.16.

Figure 3.16: Micro-Box 2000/2000c by Terasoft [8]

The Microbox-2000/2000C are suited with below specifications [8]:

a. Core™ 13-1.7 GHz
b. 8GB DDR RAM
c. 8GB SSD
d. I/O-expandability provided through standard PCI express bus
e. 6 different I/O modules including of AD, DA, Encoder, Frequency I/O and DI/O
f. Operate at 12V/24V_{DC} ± 20%

The Micro-Box 2000/2000C is a rugged, high-performance Industrial PC which is fanless, low-power and power consumption design at 41W (Typical). Besides, Micro-Box 2000/2000C allowed the Simulink Real-Time self-installed software tools to run on stand-alone mode [8]. The connection of other devices into Micro-Box are done according to the port function shown in Table 3.3.

Table 3.3: Connection port function of Micro-Box

Connector	Function	Port Number
2	AD0	1
	AD1	2
	DA0	11
	DA1	12
	ADGND	9,10
	GND	19,20
3	Encoder0 Phase A	1
	Encoder0 Phase B	2
	Encoder1 Phase A	4
	Encoder1 Phase B	5
	5V	17,18
	GND	19,20

3.3.4 Load cell

Figure 3.17: Futek Jr S Beam Load Cell with Male Thread – LRM200 FSH01672 [39]

Table 3.4: Specifications of LRM200 FSH01672[39]

Specifications	**Value**
Weight	14g (10lb/44.5N)
Safe overload	1000% of RO (100g) 200% of RO Tension only (50-100lb)
Deflection	0.004in
Natural Frequency	1700Hz

The load cell is used to measure the total force applied by an item onto it. The S-beam load cell is specifically measured the force by compressing or pulling the both end of the load cell with the two surfaces for test. In this project, a holder as shown in Figure 3.18 is created to fix the Fixed end of the load cell and to clamp it onto the mechanism.

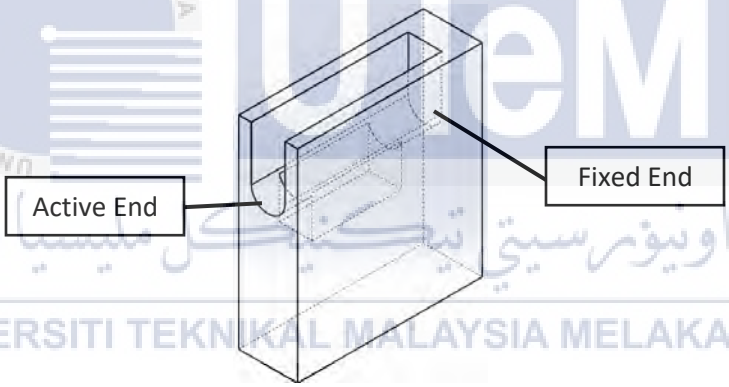

Figure 3.18: The load cell holder

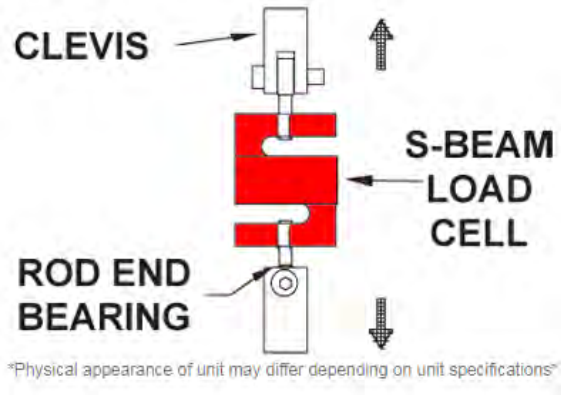

Figure 3. 19: Internal physical construction of S-beam load cell [39]

3.3.5 Wiring Connection of The Components Interfaces

According to the port function of each connector port of Micro-Box, linear encoders and the load cell shown in Table 3.2, Table 3.3 and Table 3.5, the interfaces between these devices is drawn and sent for approval from supervisor. The wiring connection is drawn as shown in Figure 3.20.

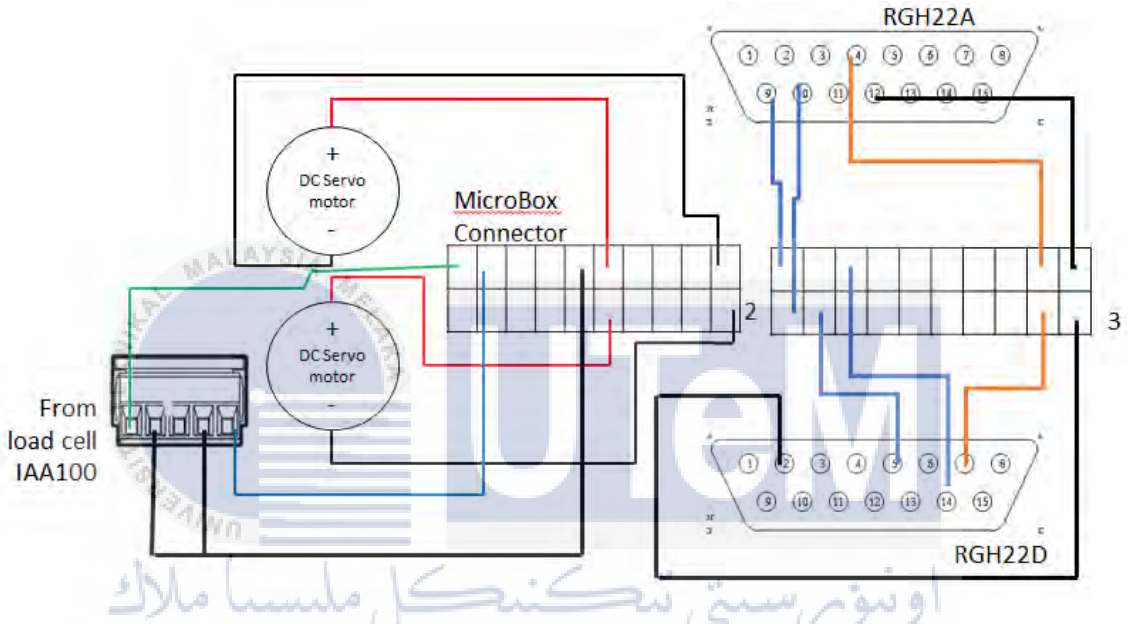

Figure 3. 20: Wiring diagram of the Twin-axes Table Drive System

3.3.6 Calibration of Linear Encoder

The linear encoder is connected to the Micro-Box for the data reading and the power supply for the linear encoder. After power up the Micro-Box, the 526sensoray encoder block that reads the data from the linear encoder is drawn in Simulink and connect to the display block and the scope to show data read. The block diagram is drawn as shown in Figure 3.21. At first, type 'xpctest' command in the command window to ensure the connectivity between MATLAB and Micro-Box is stable and compatible to each other. If the connection failed, check the configuration parameters to ensure the target to hardware is connected to xpctarget. Build the model of the Simulink block diagram that drawn before and connect it to the Micro-Box. Then, click play and manually move the ball screw

shaft of both axes to get the displacement read by the encoder. This experiment is done for 5 times to ensure the accuracy and consistency of the linear encoder function.

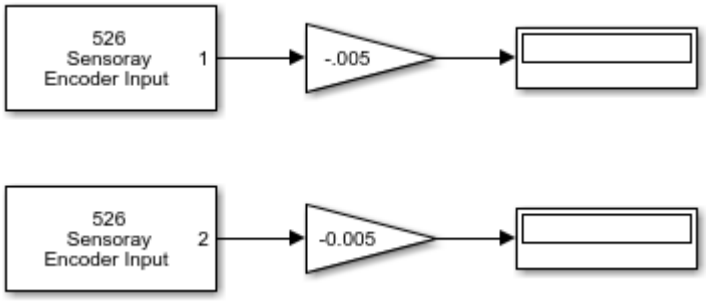

Figure 3.21: Simulink block diagram of the linear encoder calibration

3.3.7 Open-loop System Test

The connection between Micro-Box and MATLAB is done connected and all connection is done wired up as shown in Figure 3.20. The mechanical coupling is not connected in this test to prevent damages as there is no any error compensation done for the Twin Axes Table Drive System. The open loop system test is done as the configuration shown in Figure 3.22. All input values to the system is listed in Table 3.5.

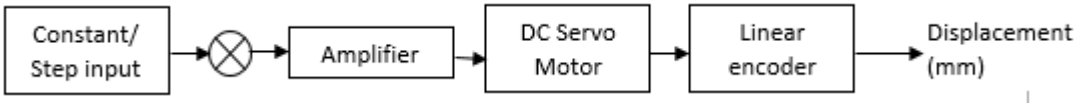

Figure 3.22: Block diagram that shows the relationship among the system during open loop.

Next, the displacement output and the velocity output are tabulated into 4 columns array data and are save from MATLAB workspace. Next, use the data saved before to draw the graph of the displacement / velocity against time by using OriginPro8 software.

Table 3.5: Input parameters to the open-loop system test

Parameters	Value	Unit
Constant input	0.5 – 1.0	(×K_{in}) mm
saturation	±20	
K_D	0.005	mm

Table 3.6: Example of table for open loop system test data collection

Time(s)	Displacement lane 1(mm)	Displacement lane 2(mm)	Velocity lane 1 (m/s)	Velocity lane 2 (m/s)
0.001				
0.002				

3.3.8 Closed-loop System Test

The wiring connection is the same as what it is done in previous experiments. During this system test, the large mover or also called as mechanical coupling is first disconnected to ensure the movement of both axes does not over mismatched to each other to prevent damages. Before started the test, block diagram for this hardware experiment is drawn to fulfil the relationship as shown in Figure 3.6 which both lanes are cross coupled at the mechanism part. The full block diagram will be show in the next chapter. As we assumed the parameters used for both lanes are the same since all components used for both axes are the same, the parameters input to the closed-loop system test for both axes are as shown in Table 3.5 stated above. The table for the data collection are still as shown as Table 3.6. Lastly, the data will be drawn into line graph with the OriginPro8 software.

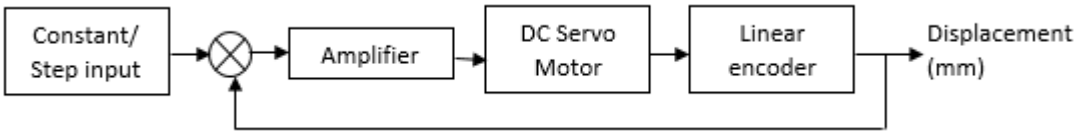

Figure 3.23: Block diagram that shows the relationship among the system during closed loop.

3.3.9 Kinematical Mathematical Modelling

The free body diagram (FBD) of singe axes ball screw is drawn and the parameters that affect the performances of the system is determined. The relationship between all these parameters is illustrated in the transfer function of the system. Figure 3.24 shows the free body diagram of single axes ball screw system and all the parameters in the system.

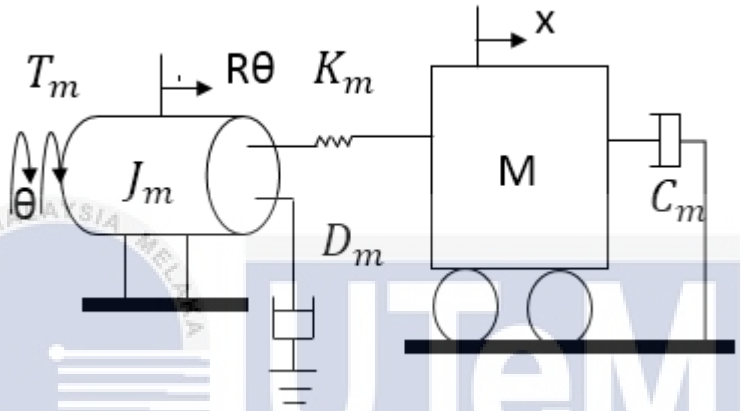

Figure3. 24: The free body diagram (FBD) of the single axis ball screw system

3.3.10 Unknown Parameters Measurement and Friction Measurement by Load Cell

Mass of the large mover (M), motor inertia (J_m), transmission ratio of the rotary to linear motion (R), rotational stiffness of screw shaft (K_m) are obtained by weighing the system and calculated with the equation for each parameter.

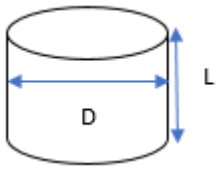

Figure 3.25: The DC motor illustration.

$$J_m = \frac{1}{4} M_m \left(\frac{D^2}{4} + \frac{L^2}{3} \right) \tag{3.1}$$

Where;

J_m = Motor inertia (kgm^2)

M_m = Mass of motor (kg)

D = Diameter of the motor (m)

L = Height of the motor (m)

Next, the load cell is used to measure the total friction force that produces between the motor and the screw shaft and the friction force occurs between the applied mass and the screw shaft which are both viscous friction that affects the performances of the real plant. As shown in Figure 3.19, it is known that when forces pulled or compressed at both end of the active and fixed end of the load cell, the total force between the surfaces are determined. Next, the total force or also known as axial force, F_a can be used to determine the friction coefficient, μ with the following equation. The position of the load cell is clamped at the position shown in Figure 3.25.

$$F_a = \mu N \tag{3.2}$$

Where;

F_a = Total force / Axial force (N)

N = Normal force = m × g

where m is the mass applied and g is the gravitational force (9.81 N)

Once the viscous friction coefficient is known, the viscous friction can be calculated with the following equation.

$$F_v = \mu N \frac{dx}{dt} \tag{3.3}$$

Where;

F_v = Viscous frictional force (N/m/sec) (Nm/rad/sec)

μ = friction coefficient

N = normal force

$\frac{dx}{dt}$ = Change in displacement over a time (m/s)

The value of parameters obtained is tabulated in table shown as Table 3.7.

Table 3.7: Parameters of Twin Axes Table Drive System (TTDS)

Parameters	Description	Value	Unit
J_m	Motor inertia		kgm^2
K_m	Rotational Stiffness of Screw Shaft		N/m
M	Mass of Table		kg
R	Transmission Ratio of Rotary to Linear Motion		m/rad
D_m	Motor Viscous Friction		Nm/rad/sec
C_m	Viscous Friction applied by mass		N/m/sec

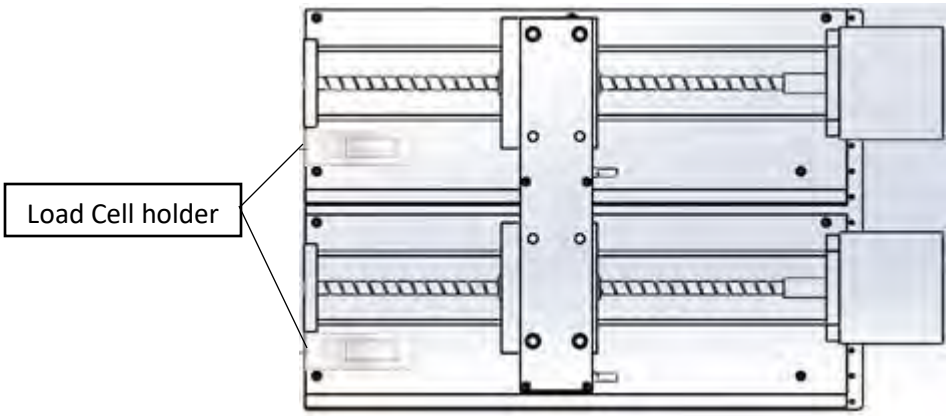

Figure 3.26: Position of load cell holder clamped

Lastly, all values are substitute into the transfer function of dual axes ball screw system block diagram that cross-coupled among the mechanical coupling is included for simulation. The performance of output displacement for the system is then analyzed.

3.4 Working Methodology During Phase 3

To achieve the third objective, a cross-coupled control system that completed with values of the parameters is constructed in system block diagram and also the transfer function. This cross-coupled control system is then constructed with a design of classic proportional control for evaluation of closed-loop performances. This controller designed will be tested in the MATLAB Simulink that gained in phase 2. The results are then compare with the results of closed-loop experiments on the dual-axes table drive system without compensation. Position tracking is the main parameters to be measured and collected.

3.4.1 Closed Loop Controller Design

The cross-coupling motion control method is applied to the real plant simulation drawn in Simulink and the output data of the simulation is collected and input to the system identification tool in MATLAB for the real plant transfer function estimation. The data is the data that without controller implementation until now.

In order to improve the performance of the Twin Axes Table Drive System (TTDS), a classical PID controller is designed with the usage of the continuous PID controller tuning method. In the PID tuner, resource response is tuned, and the step response is tuned to be the same to the resource response in order to obtain the proportional gain, K_p, derivative gain, K_D and integral gain, K_I of the system.

Lastly, the PID transfer function is then derived to have the comparison of auto tuning method and controller transfer function method. The PID controller transfer function is derived by substituting all values into the equation shown below.

$$G_{PID}(s) = K_P + \frac{K_I}{s} + \frac{K_D N}{1 + \frac{N}{s}} \tag{3.4}$$

3.5 Summary

This chapter shows the flow of the whole project and explained the mechanical and electrical devices used in construction of twin-axes table drive. Besides, the steps of simulation analysis are explained in the following section. Upon the finishing of synchronous control on twin-axes table drive system, few experiments are conducted to analysis the performance of the system.

CHAPTER 4

RESULT

4.1 Overview

This chapter present the results from experiments described in previous chapter. All results are discussed based on tabulated data in form of graphs and tables. This is aimed to analysis and understanding the occurrence of the phenomena. This chapter will explain on the modelling of the twin axes table drive system. Lastly, results that get from the experiments stated in chapter 3 are discussed.

4.2 Kinematical Mathematical Wise Modelling.

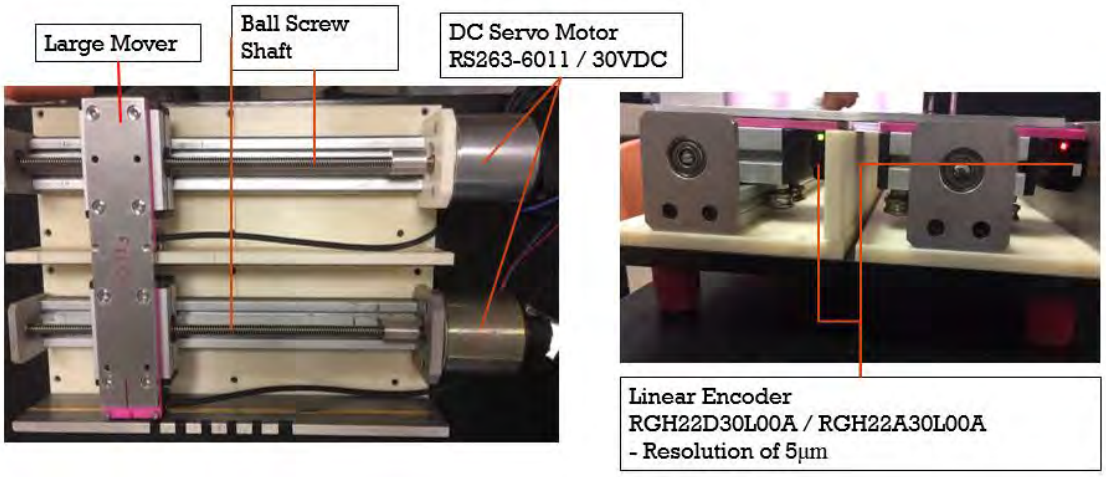

Figure 4.1: Construction of Twin Axes Table Drive System (TTDS)

To analyze the model of single axis ball screw system, translational and rotational motion of the mover and the ball screw mechanism respectively are drawn and derived from the FBD drawn below.

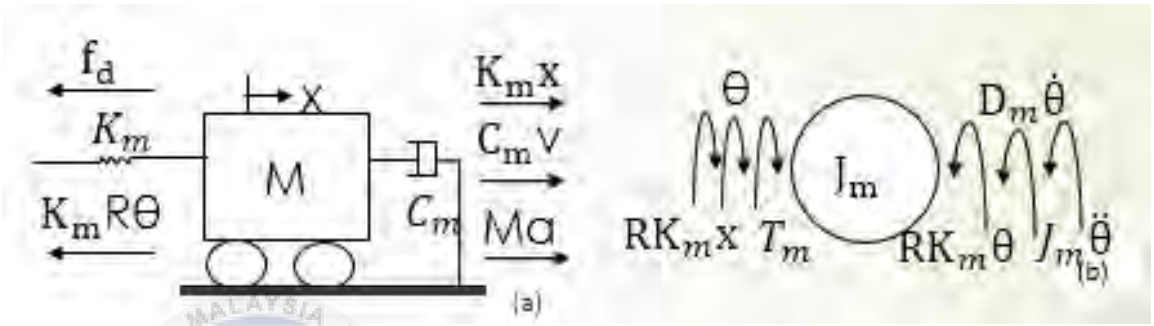

Figure 4. 2: FBD of (a) translational motion for the mover; and, (b) rotational motion of the ball screw mechanism

The transfer function for this model is derived as below for each part of motion.

For the translational motion transfer function, the transfer function of driving force onto the mover (f_d) is derived.

$$K_m\left(R\theta - x\right) + f_d = M\ddot{x} + C_m\dot{x} \tag{4.1}$$

$$f_d = MS^2X\left(s\right) + C_mSX\left(s\right) - K_mR\theta\left(s\right) + K_mX\left(s\right) \tag{4.2}$$

Where;

K_m = Rotational stiffness of ball screw shaft (N/m)

R = Transmission ratio of rotary to linear motion (m/rad)

M = Mass of the mover (kg)

C_m = Viscous friction applied by mass (N/m/sec)

Besides, the below transfer function of motor torque (Tm) that drive the rotational motion of system is derived.

$$T_m = J_m\ddot{\theta} + D_m\dot{\theta} + RK_m\left(R\theta - x\right) \tag{4.3}$$

$$T_m = J_m S^2\theta(s) + D_m S\theta(s) - K_m R\theta(s) + K_m X(s) \tag{4.4}$$

Where;

J_m = Motor inertia (kgm^2)

D_m = Viscous friction of motor (Nm/rad/sec)

From (4.2) and (4.3), the model matrix is rearranged as shown below:

$$\begin{bmatrix} T_m \\ f_d \end{bmatrix} = \begin{bmatrix} J_m S^2 + D_m S + R^2 K_m & -RK_m \\ -RK_m & MS^2 + C_m S + K_m \end{bmatrix} \begin{bmatrix} \theta \\ X \end{bmatrix} \tag{4.5}$$

For the single axis ball screw mechanism, the block diagram can be constructed as shown in Figure 4.3.

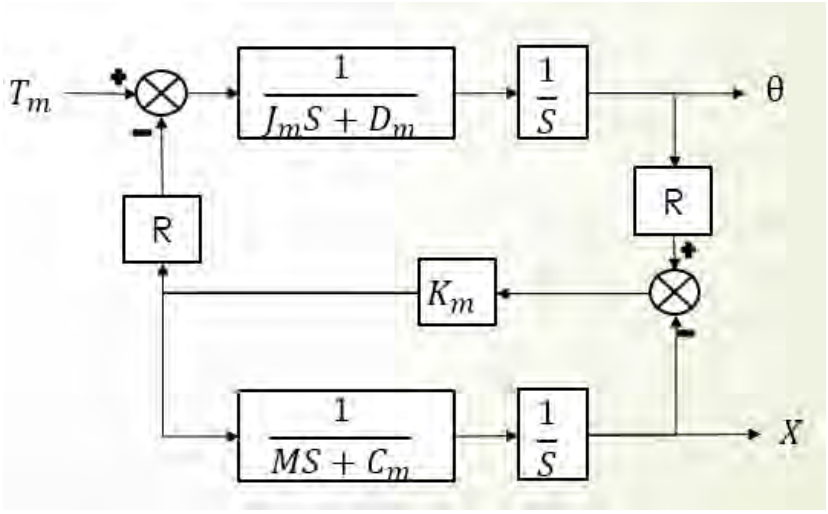

Figure 4. 3: Block diagram of the single axis ball screw mechanism

The twin axes table drive system that taking displacement, X as the output parameter is then can be constructed by included the coupling forces (f_{11}, f_{22} , f_{12}, f_{21}) that taking the torque as the input for the ball screw axis.

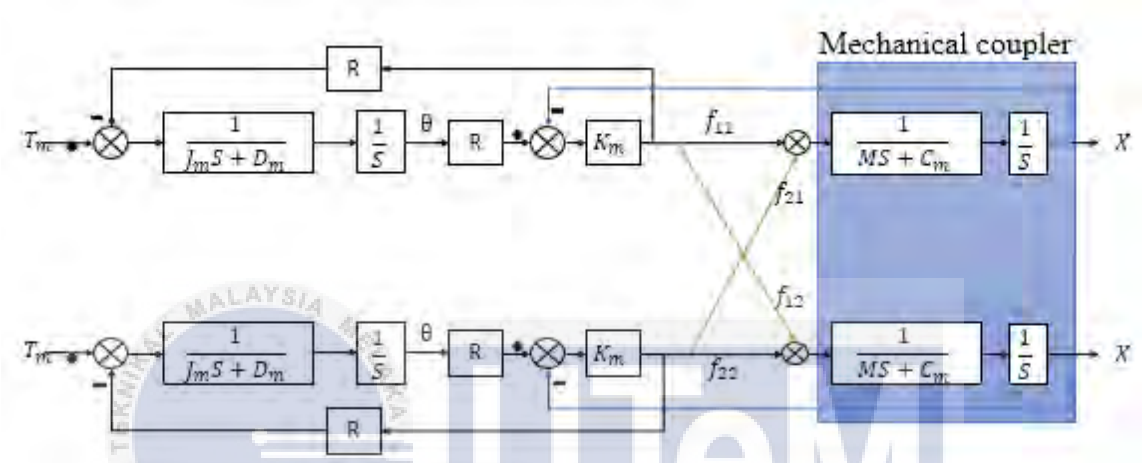

Figure 4.4: Cross-coupled control of the twin axes table drive system

4.3 Experimental results and discussion

4.3.1 Experiment 1: Linear Integration

The results of the calibrated linear encoder are tabulated and analyzed. From the specification of RGH22A series linear encoder, it has been informed that with resolution of 5µm. Next, the reading of the position by linear encoder is in millimeter (mm) where 5µm equals to 0.005mm.

Hence, a gain of 0.005 is applied into the system reading to get the results in mm as shown in Figure 4.5. Table1 shows the reading of encoder when the mover is driven by the DC servo motor at 4V step input in 10 seconds for each ball screw lanes.

Table 4.1: Calibrated reading of linear encoder

Reference point, mm	Actual reading, mm	
	Lane 1	Lane 2
210	131.380	156.415
210	125.735	157.645
210	121.965	157.700
210	127.970	159.800
210	130.165	159.235

From Table 4.1, the displacement of the actual reading for both lane is inaccurate to the measured displacement that the mover moved due to the unstable operation of the linear encoder. However, the consistency of the readings is at the standard deviation of 0 with the calculation as shown below.

$$S = \sqrt{\frac{\sum (x - \bar{x})^2}{n-1}} \tag{4.6}$$

$$S = \sqrt{\frac{\sum (x - 127.443)^2}{5-1}}$$

$$S = 0$$

4.3.2 Experiment 2: Open Loop System Test

This experiment is done by running the twin axes table drive system in open loop test and the displacement or position tracking is done. The system is run and it can be seen that the results are not synchronized.

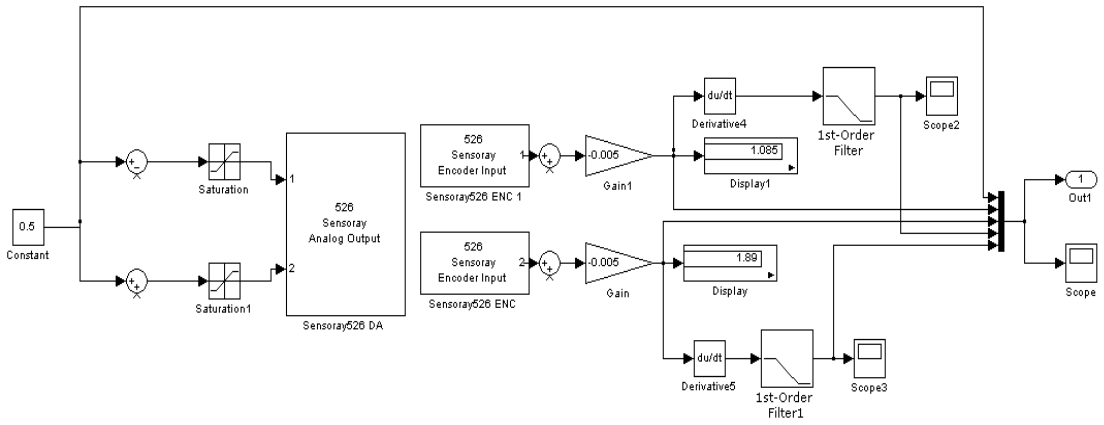

Figure 4.5: Block diagram of the open loop test for Twin Axes Table Drive System

For this experiment, there are several times of the data collected for both axes running which shows in the following Figure 4.6, Figure 4.7, Figure 4.8, Figure 4.9, and Figure 4.10 where when the constant input is given as 1 mm to 5 mm.

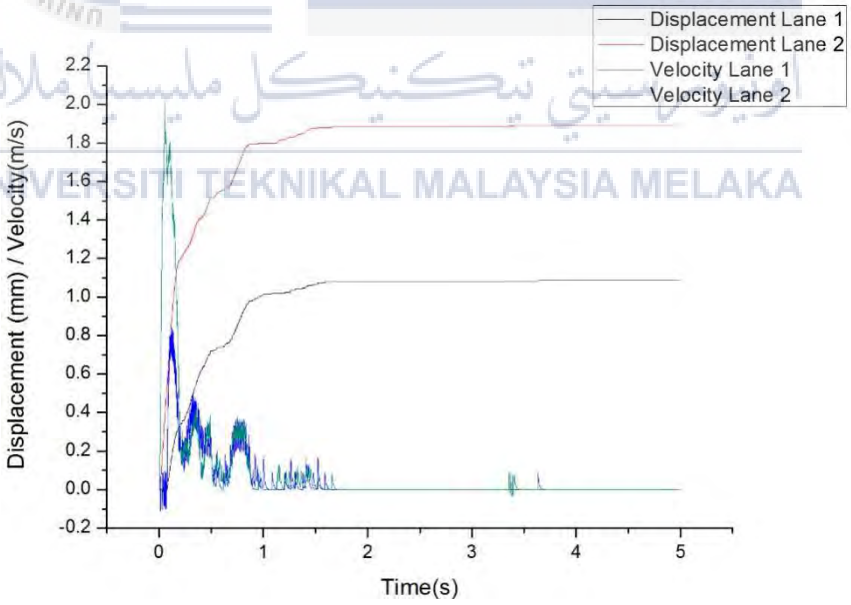

Figure 4.6: The position tracking graph of the open loop test on Twin Axes Table Drive System at 1 mm reference input

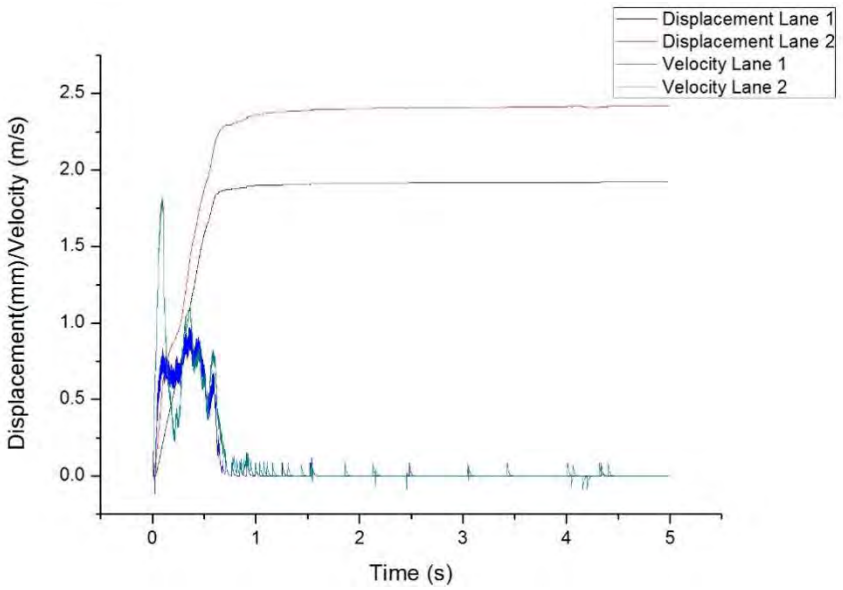

Figure 4.7: The position tracking graph of the open loop test on Twin Axes Table Drive System at 2 mm reference input

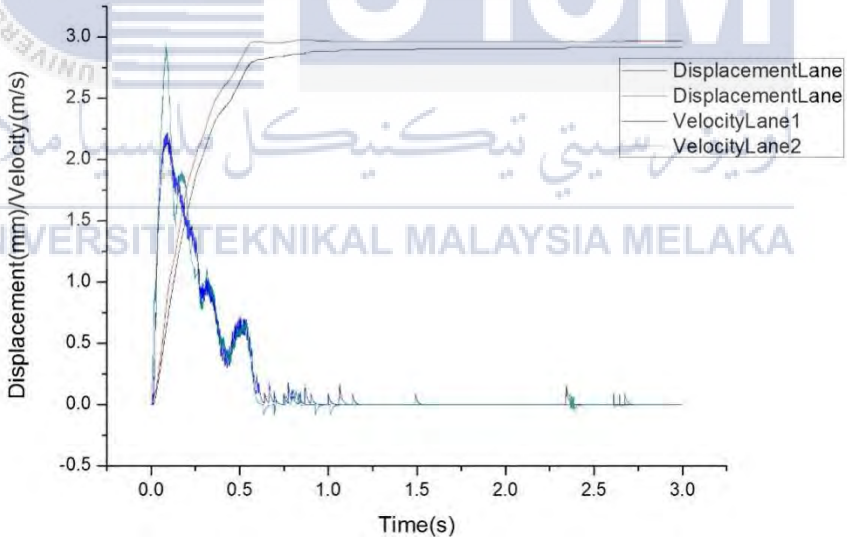

Figure 4.8: The position tracking graph of the open loop test on Twin Axes Table Drive System at 3 mm reference input

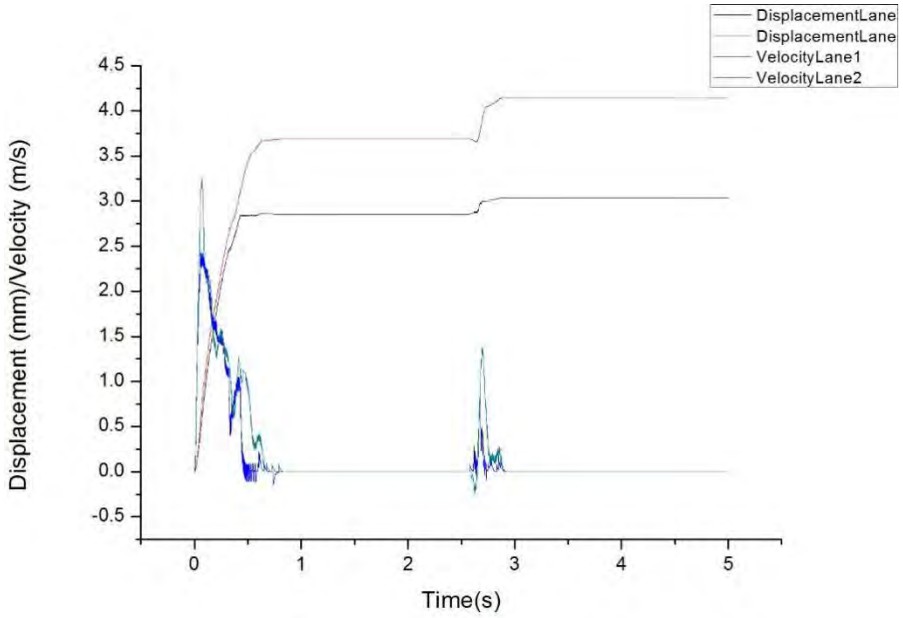

Figure 4.9: The position tracking graph of the open loop test on Twin Axes Table Drive System at 4 mm reference input

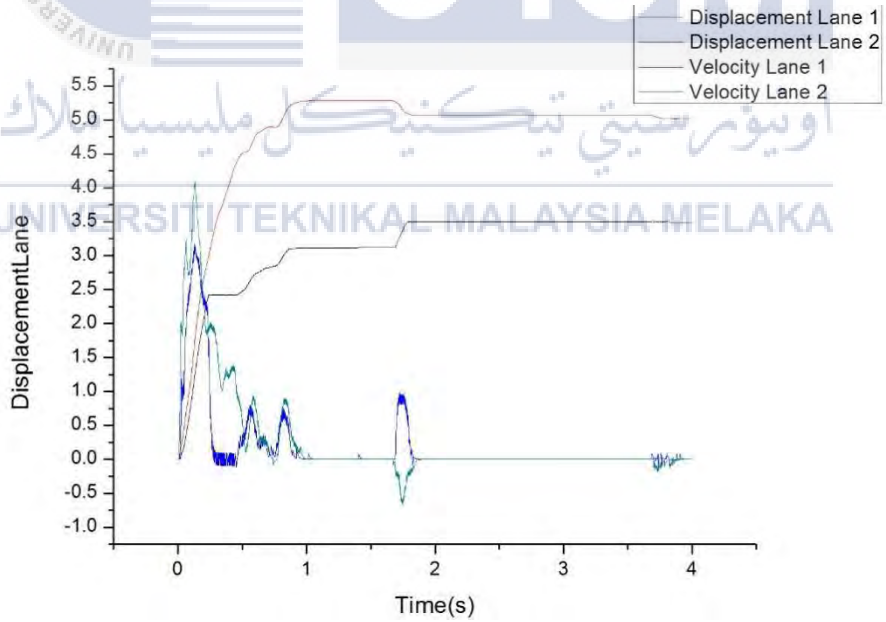

(e)

Figure 4.10: The position tracking graph of the open loop test on Twin Axes Table Drive System at 5 mm reference input

For each reference input, it can be seen that the output position for both lane does not run together in synchronize pattern. This is due to the slight bending and the stuck movement of the ball screw when the system is drive by the DC servo motor.

4.3.3 Experiment 3: Closed-loop System Test

The closed-loop block diagram of Twin Axes Table Drive System is drawn as shown in Figure 4.11 and connected to the actual hardware and the results are obtained.

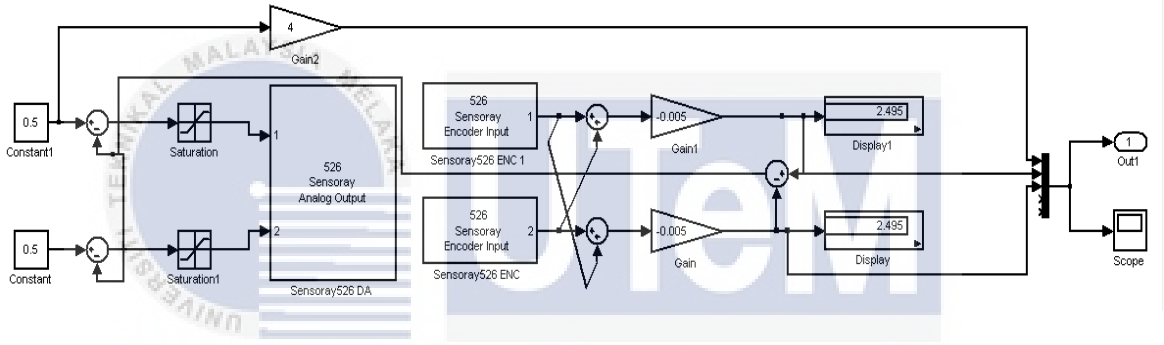

Figure 4.11: Block diagram of the closed loop test for Twin Axes Table Drive System

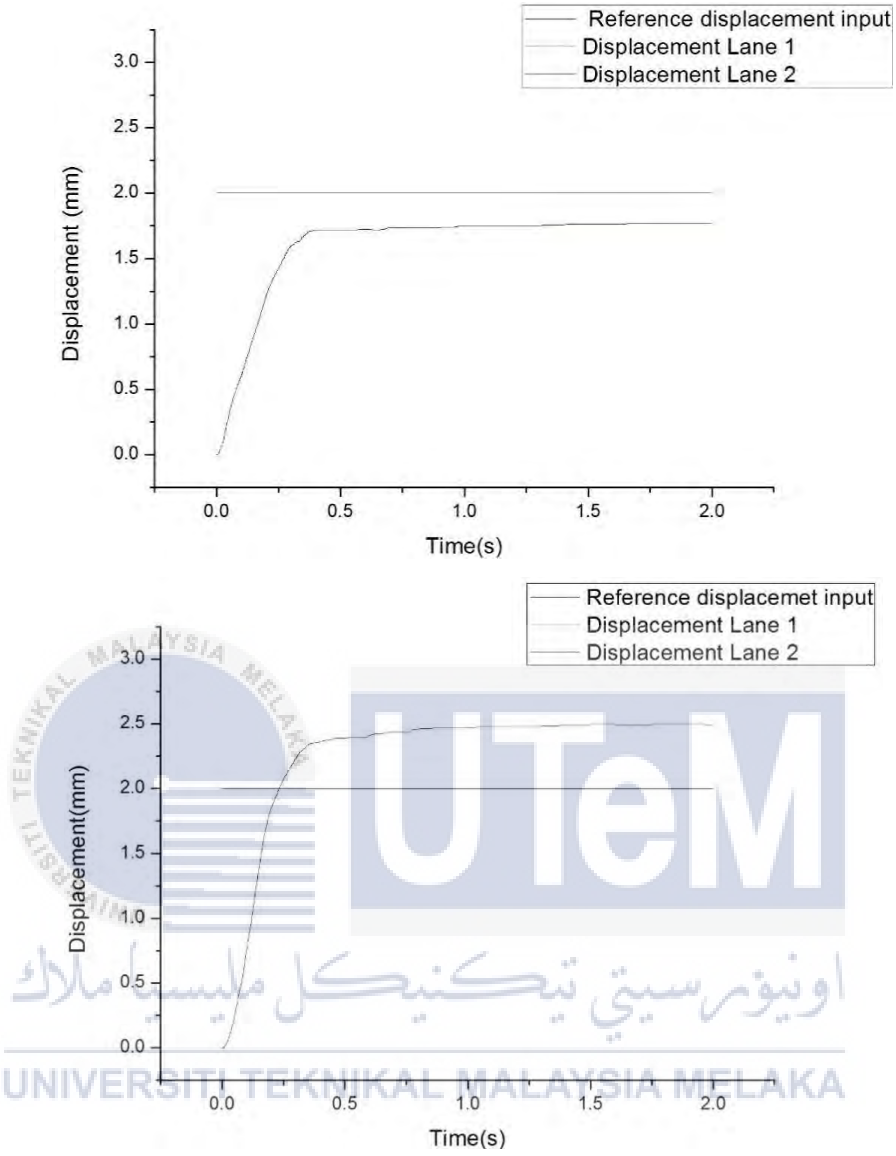

Figure 4.12: The position tracking graph of the closed loop test on Twin Axes Table Drive System at 1 mm reference input

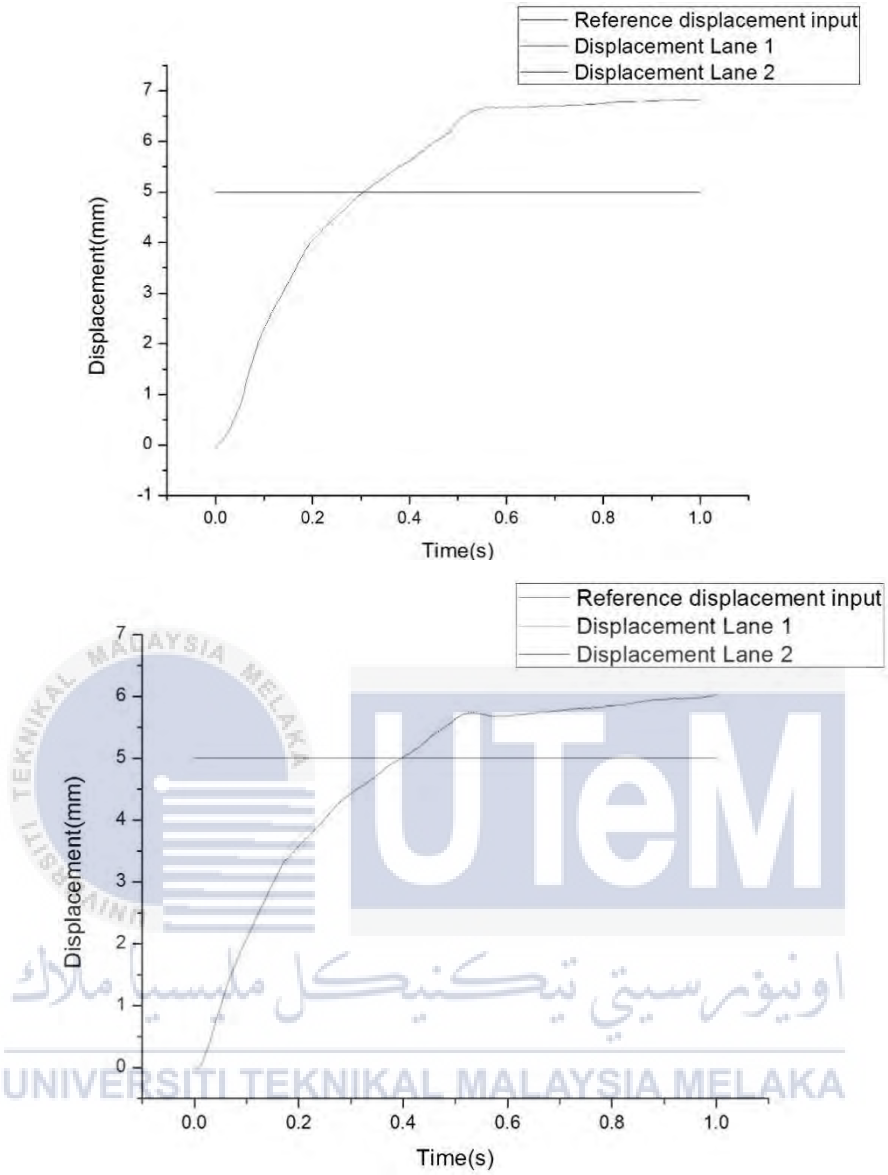

Figure 4.13: The position tracking graph of the closed loop test on Twin Axes Table Drive System at 5 mm reference input

From Figure 4.12 and Figure 4.13, it is found that both errors occurs between both lanes are compensated and the position of both lane moved are same for every single second. However, accuracy is not achieved by the cross-coupled closed loop system that designed to drive Twin Axes Table Drive System as it can be seen that the final displacement obtained is not exactly at stopped at the reference input displacement. All

data collected for the open loop system and closed loop system test are tabulated and show in Appendix C.

4.3.4 Experiment 4: Unknown Parameters Value Extraction

For the parameters that used in the transfer function for the system, some experiments are done, and data are collected. Some of the values of the parameters such as mass of the table (M), motor inertia (J_m), transmission ratio of the rotary to linear motion (R), rotational stiffness of screw shaft (K_m) are obtained from the mass weighed on the actual hardware setup.

Table 4.2: Parameters of the Twin Axes Table Drive System (TTDS)

Parameters	Description	Value	Unit
J_m	Motor inertia	6×10^{-5}	kgm^2
K_m	Rotational Stiffness of Screw Shaft	1.82×10^{3}	N/m
M	Mass of Table	6×10^{-2}	kg
R	Transmission Ratio of Rotary to Linear Motion	1.273×10^{-3}	m/rad
D_m	Motor Viscous Friction	2.0053×10^{-3}	Nm/rad/sec
C_m	Viscous Friction applied by mass	1.7026×10^{-2}	N/m/sec

The output of the load cell is in voltage mode, which 5Vdc shown is equals to 10lbs which is 44.5N. Hence, from the data collected, the total force applied by the mass is calculated with the equation as shown as below.

$$F = V \times \frac{44.5}{5} \tag{4.7}$$

Where

F = Total Force (N)

V = output voltage (V)

Each experiment data is then average as shown in the following Table4.3.

Table 4.3: Total force applied by the mass

Experiment	Force (N)	Displacement(mm)
1	0.69156	123.21
2	0.67083	128.05
3	0.688776	120.245
4	0.721105	116.945
5	0.73844	116.635
Average	0.702142	121.017

The friction coefficient is then calculated by applying the following equation.

$$\mu = \frac{F}{N} \tag{4.8}$$

where

μ = friction coefficient

F = Total force (N)

N = normal force = mass x gravitational force (9.81N)

Hence, from (4.7), it can be calculated that the friction coefficient applied by the mass is as below;

$$\mu = \frac{0.702142}{\left(6\times10^{-2}\right)\times 9.81} = 1.1929$$

$$C_m = \mu N \frac{dx}{dt} \tag{4.9}$$

$$C_m = (1.1929)(0.06\times 9.81)\left[\frac{121.245\times10^{-3}}{5}\right]$$

$$C_m = 1.7026\times10^{-2}\ {}^{N}\!/_{ms^{-1}}$$

Next, the experiment for the viscous friction of the motor is done for the value extraction. Table 4.4 shows the result of it.

Table 4.4: Total force by the motor

Experiment	Force (N)	Displacement(mm)
1	0.833235	37.6950
2	0.854644	22.0250
Average	0.84394	29.8600

$$\mu = \frac{0.84394}{\left(6\times10^{-2}\right)\times 9.81}$$

$$= 1.4338$$

$$D_m = \mu N \frac{dx}{dt}$$

$$D_m = (1.4338)(0.06 \times 9.81)\left[\frac{\left(\frac{29.86 \times 10^{-3}}{2\pi}\right)}{2}\right]$$

$$D_m = 2.0053 \times 10^{-2} Nm / rad / \sec$$

4.3.5 Experiment 5: Closed loop controller design

The closed-loop cross-coupled controller design is drawn as shown in Figure 4.14. Tracking position in mm are measured and collected in simulation. The value of parameters are set as stated in Table 4.2 for the synchronous control design drawn in Figure 4.11. The displacement output by experiment run by the real plant has been shown in Figure 4.15 which shown that the displacement output from the given input does not achieve accuracy it should have achieved.

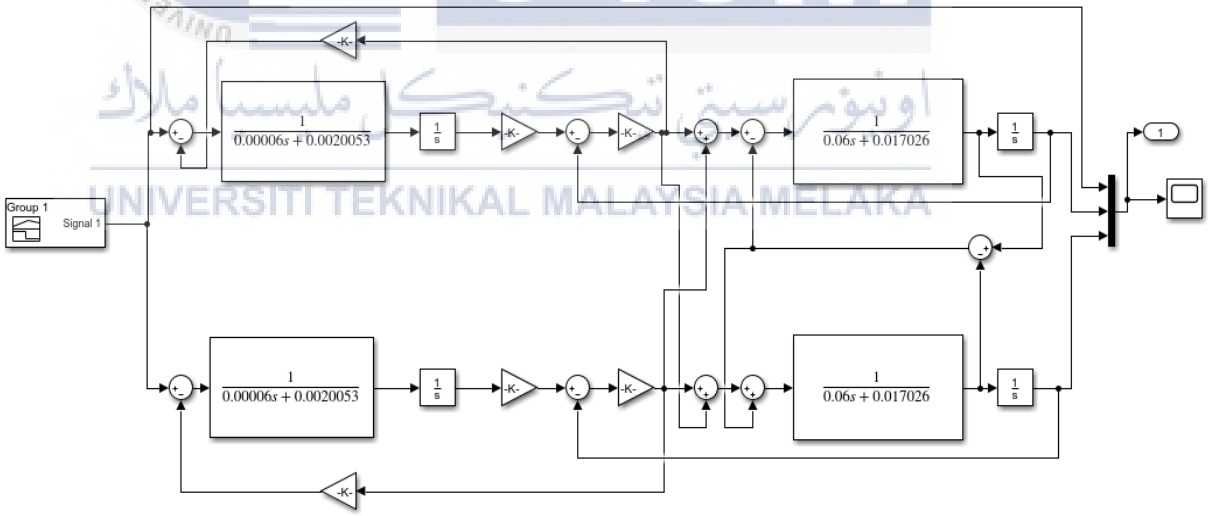

Figure 4.14: Block diagram of closed-loop cross-coupled control with compensation

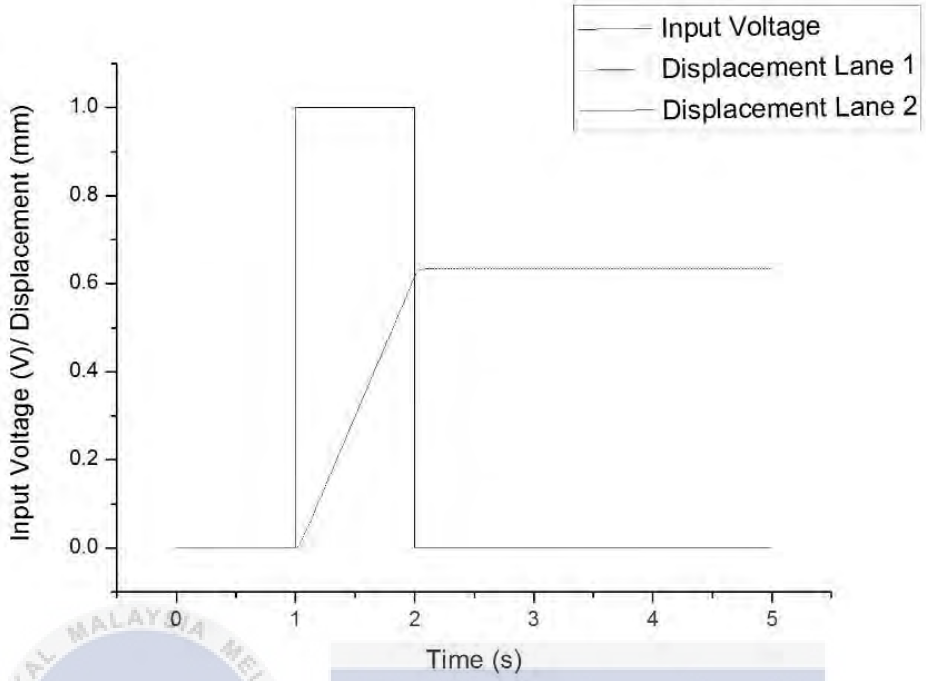

Figure 4.15: The displacement output of the closed-loop cross- coupled control system

By using the data get from the above closed loop cross-coupled control data in the system identification tools of MatLab. The transfer function is estimated as shown as following.

$$\frac{X(s)}{T(s)} = \frac{0.00423s + 4.28 \times 10^{-6}}{s^2 + 0.008416s + 5.857 \times 10^{-5}}$$

By using PID controller in Simulink, the proportional gain (K_p), integrator gain (K_I) and derivative gain (K_D) are obtained and verify with the Simulink simulation to the plant that obtained above.

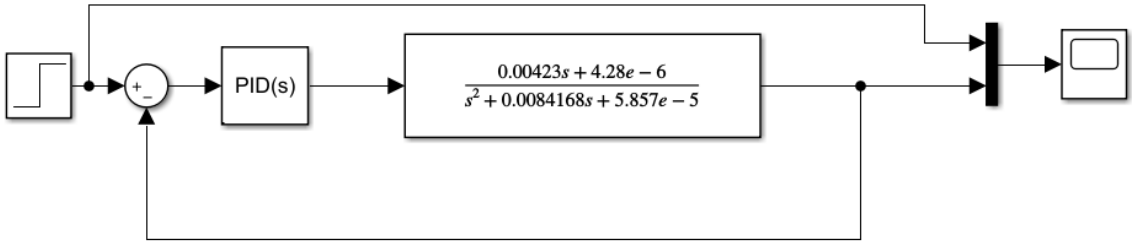

Figure 4.16: Block diagram of the PID controller design and the real plant

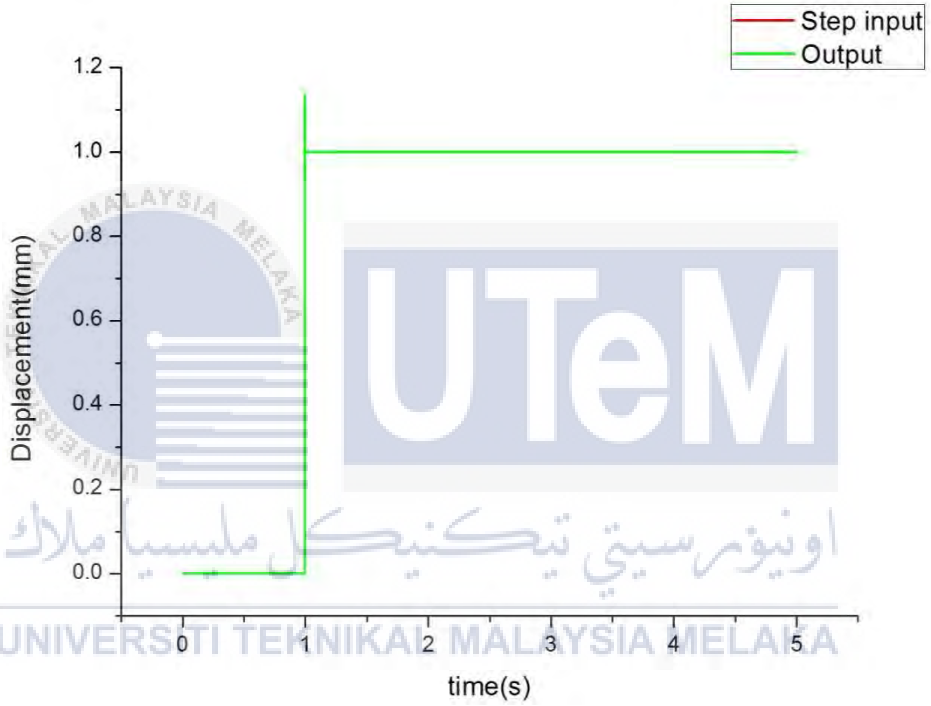

Figure 4.17: The step response of the output displacement by the plant after implementation of PID controller

The results of the gains stated above has been obtained by tuning the transient response to the most ideal step response. Values of the parameters are tabulated and shown in Table 4.5.

Table 4.5: Values of parameters for the PID controller

Parameter	Values
K_p	1.411×10^7
K_I	1.567×10^{11}
K_D	-51.20
N	9.992×10^4

From values obtained above, substitute all values into the general equation of the PID controller shown below, the transfer function of the controller will be obtained.

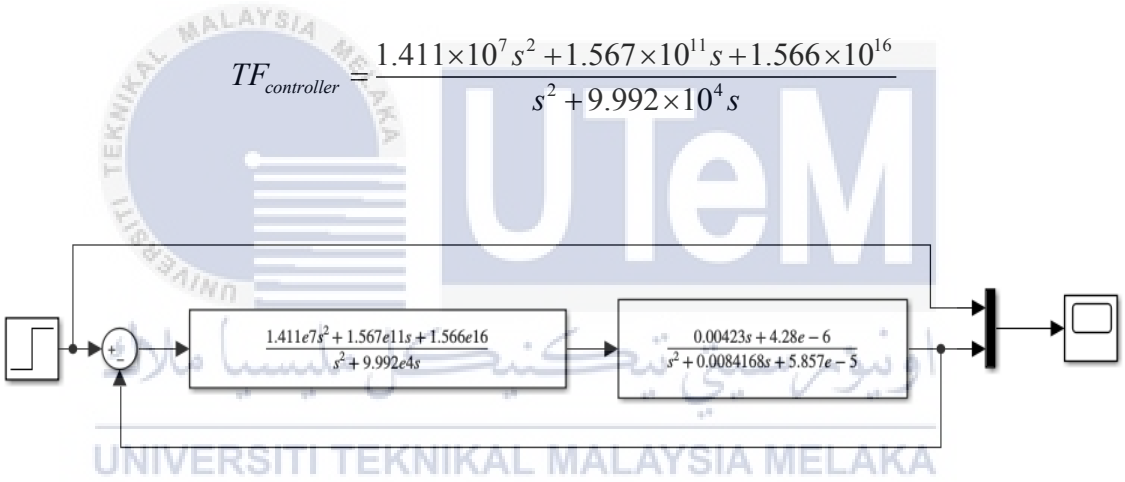

Figure 4.18: Block diagram for verification of the controller transfer function to the plant.

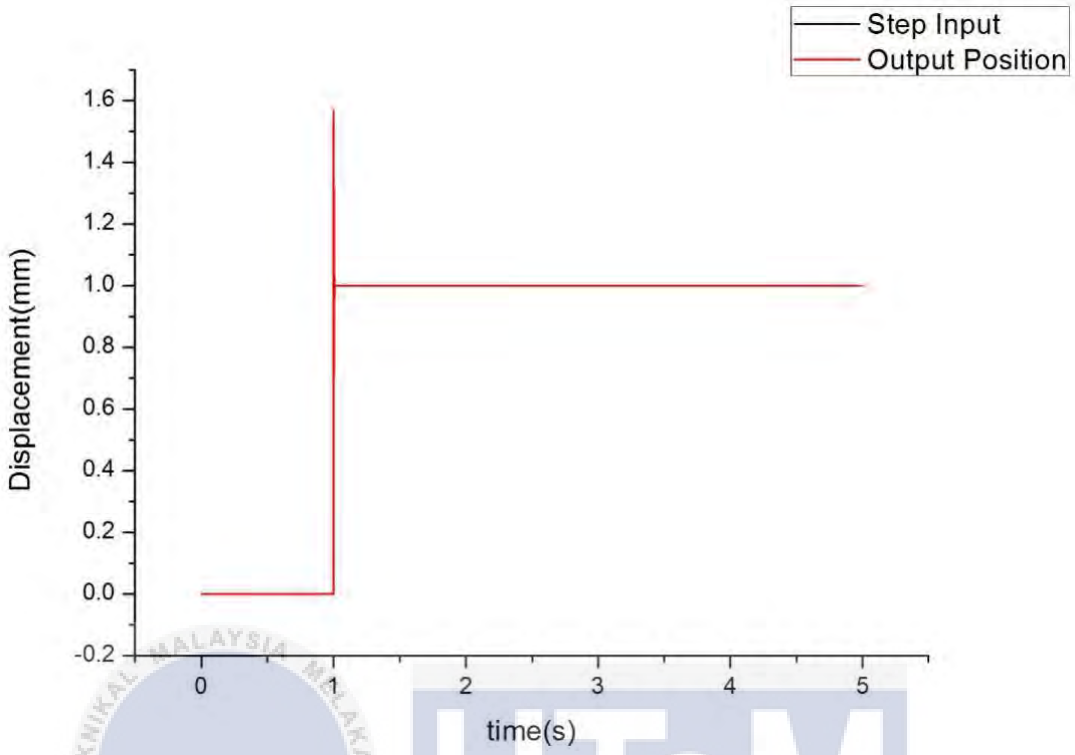

Figure 4.19: The step response of the output displacement by the plant after implementation of PID controller transfer function

According to Figure 4.17 and Figure 4.19, it can be seen that the overshoot caused by the system using the controller transfer function is higher than that of the system using auto tuning for the PID controller parameters. This is due to the accuracy of decimal places used in the transfer function derivation.

CHAPTER 5

CONCLUSION AND RECOMMENDATION

5.1 Conclusion

Synchronizing control of a twin axes table drive is a project that aimed to produce a parallelly arranged twin axes table drive that synchronously moved. In this project, focuses are mainly on the construction and modelling of the twin axes table drive system and a classic controller design that used for closed-loop performances evaluation.

Necessary procedures and scopes are well explained in this report. The procedures of the experiments are organized in flowchart and the steps. Starting of the project, researches are done for information gather and methodology decision. Researches draw the idea of the project. DC servo motor is proved to be reliable in this project although researches showed that linear motor are always used.

The hardware construction of this project has been built and run for the experiment. Before the experiment executed, the components used in this project setup has been calibrated especially the linear encoder to ensure it function well to get the position tracking results. However, the linear encoder does not function as ideal as it could be due to the slight bending occurred on the ball screw affected the movement of the table that clamped with the linear encoder to be lost with signal.

Moreover, there is position tracking between both lanes has been identified and showed in the graph for each experiment which drive with given reference input of 1mm, 2mm, 3mm, 4mm and 5mm constant input. In the closed-loop test experiment, the errors still occurred although the position tracking showed that both lanes achieve

synchronization during the running process. It can be clearly seen that the output position tracking data is not exactly same as the reference input given to the system.

Hence, a classical PID controller has been designed and verified the accuracy of the Twin Axes Table Drive System that implemented with the PID controller in simulation with MatLab Simulink. From the result, it can be concluded that the PID controller did reduce the steady state error, increase the accuracy of positioning for the plant with less overshooting occurs.

5.2 Future Works

In future, this project is recommended to be focused on the controller design for the real plant operation in order to achieve accuracy and consistency. For future improvement, it is suggested to have an advanced technology such as frictionless linear motor for this project for the improvement on the Twin Axes Table Drive System (TTDS)'s performances.

References

[1] Min-Fu Hsieh, Wu-Sung Yao, Chia-Rong Chiang, "Modeling and synchronous control of a single-axis stage driven by dual mechanically-coupled parallel ball screws", August 2007.

[2] Yunjun Chen, Xiuming Jiang, Gongyuan Yang, "Intelligent Control System for Two-motor Synchronous Driving", 2010.

[3] Zhang Chunliang, Chen Zichen, Mei Deqing, "Linear Motor Direct Drive Technology and Its Application in Machine Tools", October 2002.

[4] Carl J. Kempf and Seiichi Kobayashi, "Disturbance Observer and Feedforward Design for a High-Speed Direct-Drive Positioning Table", September 1999.

[5] National Instrument (22nd November 2017), *Data Acquisition Device,* Available: http://www.ni.com/data-acquisition/what-is/.

[6] Qingsu Wang, Gerald Barnett, R.Michael Greig, and Yi Cheng, "System and method for performing real time data acquisition, process modelling and fault detection of water fabrication processes", US 5859964 A, January 12, 1999.

[7] Joseph Rialan and Gerald Thierry, "Device for transmitting signals by radio and cable between a central control and recording system and data acquisition devices", US 4979152 A, December 18, 1990.

[8] Terasoft,Micro-Box 2200, July 2016.

[9] Yunjun Chen, Xiuming Jiang, and Gongyuan Yang, "Intelligent Control System for Two-motor Synchronous Driving", 2010.

[10] Jung-Hwan Byun and Myung-Soo Choi, "A Method of Synchronous Control System for Dual Parallel Motion Stages", June 2012.

[11] Yasafumi Yoshiura and Yasuhiko Kaku, "Synchronous Control Apparatus – US 8587 B2", 19th November 2013.

[12] Baeksuk Chu, Sungsoo Kim, Daehie Hong, Heung Keun Park and Jinmoo Park,

"Optimal Cross-Coupled Synchronizing Control of Dual-Drive Gantry System for a SMD Assembly Machine", 2004.

[13] Mi-Ching Tsai, Min-Fu Hsieh and Wu-Sung Yao, "Synchronous Control of Linear Servo Systems for CNC Machine Tools", Department of Mechanical Engineering National Cheng Kung University.

[14] Jia En Foo, Shin Horng Chong, Wai Keat Hee, Ser Lee Loh and Norhaslinda Hashim, "Fast Positioninfg Performance In Ball Screw Mechanism with Disturbance Observer",Jurnal Teknologi(Sciences & Engineering)78:8(2016) 71-7,8, 15th July, 2016.

[15] Jack Barrett, Tim Harned, Jim Monnich, "*Linear Motor Baiscs"*, Parker Hannifin Corporation.

[16] John Mouton, "*Brushed DC Motor Basics"*, Microchip.

[17] Sean DeHart, Smriti Chopra and Hannes Daepp, "Motors", unpublished.

[18] *Fleming's Left Hand Rule,* Available: https://en.wikipedia.org/wiki/Fleming%27s_left-_hand_rule_for_motors

[19] Mathworks (24th November 2017), *Mathematical Modelling – Develop and optimize mathematical models of complex systems,* Available: https://www.mathworks.com/solutions/mathematical-modeling.html

[20] *What Are Free Body Diagrams?*, Available: http://web.mit.edu/4.441/1_lectures/1_lecture14/1_lecture14.html

[21] Xiang, H., Qiu. Z., Li,X. "Simulation and Experimental Reasearch of Non-linear Friction Compensation for High-Precision Ball Screw Drive System." In The 9th International Conference on Electronic Measurement and Instruments, ICEMI 2009. Beijing, pp. 604 – 609,16 – 19 August 2009.

[22] Lorenz RD, Schmidt PB, "Synchronized Motion Control For Process Automation. In: Proceedings of the 1989 IEEE Industry Applications Annual Meeting", 1989.

[23] S.N. Huang, Y.P. Leow, H.C. Liaw, S.Y. Lim and W. Lin, "Geometrical Error Modelling and Compensation Using Neural Networks", STR-03/036/Mech.

[24] Yuxin Su, Dong Sun, Lu Ren and James K.Mills, "Integration of Saturated PI Synchronous Control and PD Feedback for Control of Parallel Manipulators",

February 2006.

[25] Po-Huan Chou, Fae-Jeng Lin, Chin-Sheng Chen and Feng-Chi Lee, "DSP-Based Cross-Coupled Synchronous Control for Dual Linear Motors via Intelligent Complementary Sliding Mode Control" in IEEE Colloqulum on Humanities,Science and Engineering Research (CHUSER 2012), 3rd December 2012.

[26] Viktor L.Orekhov, Coleman S.Knabe, Michael A.Hopkins, and Dennis W.Hong, "An Unlumped Model for Linear Series Elastic Actuators with Ball Screw Drives" in 2015 IEEE/RSJ International Conference on Intelligent Robots and Systems (IROS) Congress Center Hamburg, 28th September – 2nd October 2015.

[27] De-Peng Liu, "Parameter Idenfication For Lugre Friction Model Using Genetic Algorithms" in Proceedings of the Fifth International Conference on Machine Learning and Cybernetics, Dalian, 13rd – 16th August 2006.

[28] Karl Johan Astrom and Carlos Canudas-De-Wit, "Revisiting the LuGre Friction Model", IEEE Control Systems Magazine, December 2006.

[29] Liang Dong and WenCheng Tang, "Hybrid Modelling and Analysis of Structural Dynamic of A Ball Screw Feed Drive System", ISSN 1392-1207 Mechanika 2013, Vol. 19, no. 3, pp. 316-323, 2013.

[30] "Ball Screw Selection and Calculations" – Precision Machine Design- Ball Screw Calculations, ME EN 7960.

[31] Tony L. Schmitz, Jason E. Action, John C. Ziegert and W.Gregory Sawyer, "The Difficulty of Measuring Low Friction: Uncertainty Analysis for Friction Coefficient Measurements", Journal of Tribology, Vol. 127/673, July 2005.

[32] Ing. Jindřich Sušeň, MSc and Ing. Smolik Jan PhD., "A study on the Ball Screw Friction Torque".

[33] Hiroki Takahashi, Toru Yuki and Kyosuke Suzuki, "Modelling of Ball Screw Driven Stage for Drilling Machines with Lumped Parameter System Model and

FEM Model." JSME Mechanical Engineering Journal, Vol.3 No.4, 1st February 2016.

[34] M.Shaparuddin Bahrudin et al, "Friction Measurement System Using Load Cell for Tribotronic System on Pin-On-Disc(POD) Tribometer." in IOP Conference Series: Earth and Environmental Science, 16012114, 2013.

[35] S. Babu, K. Manisekar, and M.S. Starvin, "Experimental Investigation of Friction Effect on Liner Model Rolling Bearings for Large Diameter Thrust Bearing Design.", Tribology Industry vol. 34, no. 3, pp. 111-118, 2012.

[36] Amin Kamalzadeh, "Precision Control of High Speed Ball Screw Drives.", 2008.

[37] Carl L. Haehner, *Coefficient of Friction Measurements*, NASA Materials Engineering Branch, No.069, September 2002.

[38] Geoffrey Holroyd, "The Modelling and Correction of Ball Screw Geometric, Thermal and Load Errors on CNC Machine Tools.", 2007.

[39] *Model LRM 200 Jr S Beam Load Cell With Male Thread*, FUTEK Advenced Sensor Technology. INC.

[40] Ivan Virgala and Michal Kelemen, "Experimental Friction Identification of a DC Motor", International Journal of Mechanics and Applications 2013, vol. 3, no. 1, pp. 26 – 30, 2013.

[41] Ivan Virgala, Peter Frankovsky and Maria Kenderova, "Friction Effect Analysis of a DC Motor", American Hournal of Mechanical Engineering 2013, vol. 1, no. 1, pp. 1-5, December 2012.

[42] *Model IAA100 Analog Amplifier with Voltage Output*, FUTEK Advenced Sensor Technology. INC.

APPENDICES

APPENDIX A

MatLab Code for data extraction:

```
t=tg.timelog;
%input= tg.outputlog(:,3);
input=tg.outputlog (:,1);
d= tg.outputlog(:,2);
d1 = tg.outputlog(:,3);
v=tg.outputlog(:,4);
v1=tg.outputlog(:,5);
%a1 = tg.outputlog(:,5);
figure(1)
plot(t,input);
hold
plot(t,d,'r');
plot(t,d1,'g');
plot(t,v,'b');
plot(t,v1,'m');
data = [t input d d1 v v1]
save ('1mm1.dat','data','-ascii','-tabs')
```

MatLab code to obtain the root locus, pole zero map of transfer function:

```
g = tf([0.6559 -0.9396 0.1923 -2.797e-9],[1 0.4063 0.1923 9.151e-6]);
figure(1)
rlocus(g)
figure(2)
step(g)
figure(3)
pzmap(g)
S = stepinfo(g)
```

APPENDIX B

Analysis data for the transfer function estimation:

Iteration	Cost	Norm of step	First-order optimality	Improvement (%) Expected	Improvement (%) Achieved	Bisections
0	0.000602588	-	1.49e+08	1.19e+05	-	-
1	0.000494271	10.5	1.97e+07	1.19e+05	18	0
2	0.000481445	2.92	5.8e+06	1.45e+05	2.6	0
3	0.000480642	0.594	6.86e+04	1.45e+05	0.167	0
4	0.000480561	0.222	7.94e+03	1.46e+05	0.0168	0
5	0.000480552	0.0712	2.43e+03	1.46e+05	0.00194	0
6	0.000480551	0.0242	667	1.46e+05	0.000216	0
7	0.000480551	0.0081	235	1.46e+05	2.45e-05	0
8	0.000480551	0.00273	77.5	1.46e+05	2.76e-06	0
9	0.000480551	0.000915	26.2	1.46e+05	3.11e-07	0
10	0.000480551	0.000307	8.77	1.46e+05	3.5e-08	0
11	0.000480551	0.000103	2.95	1.46e+05	3.95e-09	0
12	0.000480551	3.46e-05	0.989	1.46e+05	4.45e-10	0
13	0.000480551	1.16e-05	0.332	1.46e+05	5.1e-11	0
14	0.000480551	3.91e-06	0.112	1.46e+05	4.43e-12	0
15	0.000480551	1.31e-06	0.0375	1.46e+05	1.29e-12	0
16	0.000480551	4.4e-07	0.0125	1.46e+05	1.47e-13	0
17	0.000480551	1.48e-07	0.00593	1.46e+05	3.38e-14	0
18	0.000480551	4.97e-08	0.00593	1.46e+05	4.06e-13	0
19	0.000480551	1.67e-08	0.00593	1.46e+05	1.35e-13	0
20	0.000480551	5.6e-09	0.00593	1.46e+05	6.54e-13	0

APPENDIXC

Sample of the displacement data of the open loop system test:

Time(s)	d1	d2	v1	v2
3.7	2.26	4.425	3.12E-103	1.02E-10
3.701	2.26	4.425	2.87E-103	9.39E-11
3.702	2.26	4.425	2.64E-103	8.64E-11
3.703	2.26	4.425	2.43E-103	7.95E-11
3.704	2.26	4.425	2.24E-103	7.31E-11
3.705	2.26	4.425	2.06E-103	6.73E-11
3.706	2.26	4.425	1.89E-103	6.19E-11
3.707	2.26	4.425	1.74E-103	5.70E-11
3.708	2.26	4.425	1.60E-103	5.24E-11
3.709	2.26	4.425	1.47E-103	4.82E-11
3.71	2.26	4.425	1.36E-103	4.44E-11
3.711	2.26	4.425	1.25E-103	4.08E-11
3.712	2.26	4.425	1.15E-103	3.75E-11
3.713	2.26	4.425	1.06E-103	3.45E-11
3.714	2.26	4.425	9.72E-104	3.18E-11
3.715	2.26	4.425	8.94E-104	2.92E-11
3.716	2.26	4.425	8.23E-104	2.69E-11
3.717	2.26	4.425	7.57E-104	2.48E-11
3.718	2.26	4.425	6.97E-104	2.28E-11
3.719	2.26	4.425	6.41E-104	2.10E-11
3.72	2.26	4.425	5.90E-104	1.93E-11
3.721	2.26	4.425	5.42E-104	1.77E-11
3.722	2.26	4.425	4.99E-104	1.63E-11
3.723	2.26	4.425	4.59E-104	1.50E-11
3.724	2.26	4.425	4.22E-104	1.38E-11
3.725	2.26	4.425	3.89E-104	1.27E-11
3.726	2.26	4.425	3.58E-104	1.17E-11
3.727	2.26	4.425	3.29E-104	1.08E-11
3.728	2.26	4.425	3.03E-104	9.90E-12
3.729	2.26	4.425	2.78E-104	9.11E-12
3.73	2.26	4.425	2.56E-104	8.38E-12
3.731	2.26	4.425	2.36E-104	7.71E-12
3.732	2.26	4.425	2.17E-104	7.09E-12
3.733	2.26	4.425	2.00E-104	6.52E-12
3.734	2.26	4.425	1.84E-104	6.00E-12

3.735	2.26	4.425	1.69E-104	5.52E-12
3.736	2.26	4.425	1.55E-104	5.08E-12
3.737	2.26	4.425	1.43E-104	4.67E-12
3.738	2.26	4.425	1.32E-104	4.30E-12
3.739	2.26	4.425	1.21E-104	3.96E-12
3.74	2.26	4.425	1.11E-104	3.64E-12
3.741	2.26	4.425	1.02E-104	3.35E-12
3.742	2.26	4.425	9.43E-105	3.08E-12
3.743	2.26	4.425	8.67E-105	2.84E-12
3.744	2.26	4.425	7.98E-105	2.61E-12
3.745	2.26	4.425	7.34E-105	2.40E-12
3.746	2.26	4.425	6.75E-105	2.21E-12
3.747	2.26	4.425	6.21E-105	2.03E-12
3.748	2.26	4.425	5.72E-105	1.87E-12
3.749	2.26	4.425	5.26E-105	1.72E-12
3.75	2.26	4.425	4.84E-105	1.58E-12
3.751	2.26	4.425	4.45E-105	1.46E-12
3.752	2.26	4.425	4.10E-105	1.34E-12
3.753	2.26	4.425	3.77E-105	1.23E-12
3.754	2.26	4.425	3.47E-105	1.13E-12
3.755	2.26	4.425	3.19E-105	1.04E-12
3.756	2.26	4.425	2.94E-105	9.60E-13
3.757	2.26	4.425	2.70E-105	8.83E-13
3.758	2.26	4.425	2.48E-105	8.12E-13
3.759	2.26	4.425	2.29E-105	7.47E-13
3.76	2.26	4.425	2.10E-105	6.88E-13
3.761	2.26	4.425	1.93E-105	6.33E-13
3.762	2.26	4.425	1.78E-105	5.82E-13
3.763	2.26	4.425	1.64E-105	5.35E-13
3.764	2.26	4.425	1.51E-105	4.93E-13
3.765	2.26	4.425	1.39E-105	4.53E-13
3.766	2.26	4.425	1.28E-105	4.17E-13
3.767	2.26	4.425	1.17E-105	3.84E-13
3.768	2.26	4.425	1.08E-105	3.53E-13
3.769	2.26	4.425	9.93E-106	3.25E-13
3.77	2.26	4.425	9.14E-106	2.99E-13
3.771	2.26	4.425	8.41E-106	2.75E-13
3.772	2.26	4.425	7.74E-106	2.53E-13
3.773	2.26	4.425	7.12E-106	2.33E-13
3.774	2.26	4.425	6.55E-106	2.14E-13
3.775	2.26	4.425	6.03E-106	1.97E-13

3.776	2.26	4.425	5.54E-106	1.81E-13
3.777	2.26	4.425	5.10E-106	1.67E-13
3.778	2.26	4.425	4.69E-106	1.53E-13
3.779	2.26	4.425	4.32E-106	1.41E-13
3.78	2.26	4.425	3.97E-106	1.30E-13
3.781	2.26	4.425	3.65E-106	1.19E-13
3.782	2.26	4.425	3.36E-106	1.10E-13
3.783	2.26	4.425	3.09E-106	1.01E-13
3.784	2.26	4.425	2.85E-106	9.30E-14
3.785	2.26	4.425	2.62E-106	8.56E-14
3.786	2.26	4.425	2.41E-106	7.88E-14
3.787	2.26	4.425	2.22E-106	7.25E-14
3.788	2.26	4.425	2.04E-106	6.67E-14
3.789	2.26	4.425	1.88E-106	6.13E-14
3.79	2.26	4.425	1.73E-106	5.64E-14
3.791	2.26	4.425	1.59E-106	5.19E-14
3.792	2.26	4.425	1.46E-106	4.78E-14
3.793	2.26	4.425	1.34E-106	4.40E-14
3.794	2.26	4.425	1.24E-106	4.04E-14
3.795	2.26	4.425	1.14E-106	3.72E-14
3.796	2.26	4.425	1.05E-106	3.42E-14
3.797	2.26	4.425	9.63E-107	3.15E-14
3.798	2.26	4.425	8.86E-107	2.90E-14
3.799	2.26	4.425	8.15E-107	2.67E-14
3.8	2.26	4.425	7.50E-107	2.45E-14
3.801	2.26	4.425	6.90E-107	2.26E-14
3.802	2.26	4.425	6.35E-107	2.08E-14
3.803	2.26	4.425	5.84E-107	1.91E-14
3.804	2.26	4.425	5.38E-107	1.76E-14
3.805	2.26	4.425	4.95E-107	1.62E-14
3.806	2.26	4.425	4.55E-107	1.49E-14
3.807	2.26	4.425	4.19E-107	1.37E-14
3.808	2.26	4.425	3.85E-107	1.26E-14
3.809	2.26	4.425	3.54E-107	1.16E-14
3.81	2.26	4.425	3.26E-107	1.07E-14
3.811	2.26	4.425	3.00E-107	9.81E-15
3.812	2.26	4.425	2.76E-107	9.02E-15
3.813	2.26	4.425	2.54E-107	8.30E-15
3.814	2.26	4.425	2.34E-107	7.64E-15
3.815	2.26	4.425	2.15E-107	7.03E-15
3.816	2.26	4.425	1.98E-107	6.46E-15

3.817	2.26	4.425	1.82E-107	5.95E-15
3.818	2.26	4.425	1.67E-107	5.47E-15
3.819	2.26	4.425	1.54E-107	5.03E-15
3.82	2.26	4.425	1.42E-107	4.63E-15
3.821	2.26	4.425	1.30E-107	4.26E-15
3.822	2.26	4.425	1.20E-107	3.92E-15
3.823	2.26	4.425	1.10E-107	3.61E-15
3.824	2.26	4.425	1.02E-107	3.32E-15
3.825	2.26	4.425	9.34E-108	3.05E-15
3.826	2.26	4.425	8.59E-108	2.81E-15
3.827	2.26	4.425	7.91E-108	2.58E-15
3.828	2.26	4.425	7.27E-108	2.38E-15
3.829	2.26	4.425	6.69E-108	2.19E-15
3.83	2.26	4.425	6.16E-108	2.01E-15
3.831	2.26	4.425	5.67E-108	1.85E-15
3.832	2.26	4.425	5.21E-108	1.70E-15
3.833	2.26	4.425	4.80E-108	1.57E-15
3.834	2.26	4.425	4.41E-108	1.44E-15
3.835	2.26	4.425	4.06E-108	1.33E-15
3.836	2.26	4.425	3.73E-108	1.22E-15
3.837	2.26	4.425	3.44E-108	1.12E-15
3.838	2.26	4.425	3.16E-108	1.03E-15
3.839	2.26	4.425	2.91E-108	9.51E-16
3.84	2.26	4.425	2.68E-108	8.75E-16
3.841	2.26	4.425	2.46E-108	8.05E-16
3.842	2.26	4.425	2.27E-108	7.41E-16
3.843	2.26	4.425	2.08E-108	6.81E-16
3.844	2.26	4.425	1.92E-108	6.27E-16
3.845	2.26	4.425	1.76E-108	5.77E-16
3.846	2.26	4.425	1.62E-108	5.31E-16
3.847	2.26	4.425	1.49E-108	4.88E-16
3.848	2.26	4.425	1.37E-108	4.49E-16
3.849	2.26	4.425	1.26E-108	4.13E-16
3.85	2.26	4.425	1.16E-108	3.80E-16
3.851	2.26	4.425	1.07E-108	3.50E-16
3.852	2.26	4.425	9.84E-109	3.22E-16
3.853	2.26	4.425	9.06E-109	2.96E-16
3.854	2.26	4.425	8.33E-109	2.72E-16
3.855	2.26	4.425	7.67E-109	2.51E-16
3.856	2.26	4.425	7.05E-109	2.31E-16
3.857	2.26	4.425	6.49E-109	2.12E-16

3.858	2.26	4.425	5.97E-109	1.95E-16
3.859	2.26	4.425	5.49E-109	1.80E-16
3.86	2.26	4.425	5.05E-109	1.65E-16
3.861	2.26	4.425	4.65E-109	1.52E-16
3.862	2.26	4.425	4.28E-109	1.40E-16
3.863	2.26	4.425	3.94E-109	1.29E-16
3.864	2.26	4.425	3.62E-109	1.18E-16
3.865	2.26	4.425	3.33E-109	1.09E-16
3.866	2.26	4.425	3.07E-109	1.00E-16
3.867	2.26	4.425	2.82E-109	9.22E-17
3.868	2.26	4.425	2.59E-109	8.48E-17
3.869	2.26	4.425	2.39E-109	7.81E-17
3.87	2.26	4.425	2.20E-109	7.18E-17
3.871	2.26	4.425	2.02E-109	6.61E-17
3.872	2.26	4.425	1.86E-109	6.08E-17
3.873	2.26	4.425	1.71E-109	5.59E-17
3.874	2.26	4.425	1.57E-109	5.15E-17
3.875	2.26	4.425	1.45E-109	4.73E-17
3.876	2.26	4.425	1.33E-109	4.36E-17
3.877	2.26	4.425	1.23E-109	4.01E-17
3.878	2.26	4.425	1.13E-109	3.69E-17
3.879	2.26	4.425	1.04E-109	3.39E-17
3.88	2.26	4.425	9.55E-110	3.12E-17
3.881	2.26	4.425	8.78E-110	2.87E-17
3.882	2.26	4.425	8.08E-110	2.64E-17
3.883	2.26	4.425	7.43E-110	2.43E-17
3.884	2.26	4.425	6.84E-110	2.24E-17
3.885	2.26	4.425	6.29E-110	2.06E-17
3.886	2.26	4.425	5.79E-110	1.89E-17
3.887	2.26	4.425	5.33E-110	1.74E-17
3.888	2.26	4.425	4.90E-110	1.60E-17
3.889	2.26	4.425	4.51E-110	1.47E-17
3.89	2.26	4.425	4.15E-110	1.36E-17
3.891	2.26	4.425	3.82E-110	1.25E-17
3.892	2.26	4.425	3.51E-110	1.15E-17
3.893	2.26	4.425	3.23E-110	1.06E-17
3.894	2.26	4.425	2.97E-110	9.72E-18
3.895	2.26	4.425	2.73E-110	8.94E-18
3.896	2.26	4.425	2.52E-110	8.23E-18
3.897	2.26	4.425	2.31E-110	7.57E-18
3.898	2.26	4.425	2.13E-110	6.96E-18

3.899	2.26	4.425	1.96E-110	6.41E-18
3.9	2.26	4.425	1.80E-110	5.89E-18
3.901	2.26	4.425	1.66E-110	5.42E-18
3.902	2.26	4.425	1.53E-110	4.99E-18
3.903	2.26	4.425	1.40E-110	4.59E-18
3.904	2.26	4.425	1.29E-110	4.22E-18
3.905	2.26	4.425	1.19E-110	3.89E-18
3.906	2.26	4.425	1.09E-110	3.57E-18
3.907	2.26	4.425	1.01E-110	3.29E-18
3.908	2.26	4.425	9.26E-111	3.03E-18
3.909	2.26	4.425	8.52E-111	2.78E-18
3.91	2.26	4.425	7.83E-111	2.56E-18
3.911	2.26	4.425	7.21E-111	2.36E-18
3.912	2.26	4.425	6.63E-111	2.17E-18
3.913	2.26	4.425	6.10E-111	1.99E-18
3.914	2.26	4.425	5.61E-111	1.84E-18
3.915	2.26	4.425	5.17E-111	1.69E-18
3.916	2.26	4.425	4.75E-111	1.55E-18
3.917	2.26	4.425	4.37E-111	1.43E-18
3.918	2.26	4.425	4.02E-111	1.32E-18
3.919	2.26	4.425	3.70E-111	1.21E-18
3.92	2.26	4.425	3.40E-111	1.11E-18
3.921	2.26	4.425	3.13E-111	1.02E-18
3.922	2.26	4.425	2.88E-111	9.42E-19
3.923	2.26	4.425	2.65E-111	8.67E-19
3.924	2.26	4.425	2.44E-111	7.98E-19
3.925	2.26	4.425	2.24E-111	7.34E-19
3.926	2.26	4.425	2.07E-111	6.75E-19
3.927	2.26	4.425	1.90E-111	6.21E-19
3.928	2.26	4.425	1.75E-111	5.72E-19
3.929	2.26	4.425	1.61E-111	5.26E-19
3.93	2.26	4.425	1.48E-111	4.84E-19
3.931	2.26	4.425	1.36E-111	4.45E-19
3.932	2.26	4.425	1.25E-111	4.10E-19
3.933	2.26	4.425	1.15E-111	3.77E-19
3.934	2.26	4.425	1.06E-111	3.47E-19
3.935	2.26	4.425	9.76E-112	3.19E-19
3.936	2.26	4.425	8.98E-112	2.93E-19
3.937	2.26	4.425	8.26E-112	2.70E-19
3.938	2.26	4.425	7.60E-112	2.48E-19
3.939	2.26	4.425	6.99E-112	2.29E-19

3.94	2.26	4.425	6.43E-112	2.10E-19
3.941	2.26	4.425	5.92E-112	1.93E-19
3.942	2.26	4.425	5.44E-112	1.78E-19
3.943	2.26	4.425	5.01E-112	1.64E-19
3.944	2.26	4.425	4.61E-112	1.51E-19
3.945	2.26	4.425	4.24E-112	1.39E-19
3.946	2.26	4.425	3.90E-112	1.28E-19
3.947	2.26	4.425	3.59E-112	1.17E-19
3.948	2.26	4.425	3.30E-112	1.08E-19
3.949	2.26	4.425	3.04E-112	9.93E-20
3.95	2.26	4.425	2.79E-112	9.14E-20
3.951	2.26	4.425	2.57E-112	8.41E-20
3.952	2.26	4.425	2.37E-112	7.73E-20
3.953	2.26	4.425	2.18E-112	7.12E-20
3.954	2.26	4.425	2.00E-112	6.55E-20
3.955	2.26	4.425	1.84E-112	6.02E-20
3.956	2.26	4.425	1.70E-112	5.54E-20
3.957	2.26	4.425	1.56E-112	5.10E-20
3.958	2.26	4.425	1.43E-112	4.69E-20
3.959	2.26	4.425	1.32E-112	4.32E-20
3.96	2.26	4.425	1.21E-112	3.97E-20
3.961	2.26	4.425	1.12E-112	3.65E-20
3.962	2.26	4.425	1.03E-112	3.36E-20
3.963	2.26	4.425	9.46E-113	3.09E-20
3.964	2.26	4.425	8.70E-113	2.85E-20
3.965	2.26	4.425	8.01E-113	2.62E-20
3.966	2.26	4.425	7.37E-113	2.41E-20
3.967	2.26	4.425	6.78E-113	2.22E-20
3.968	2.26	4.425	6.24E-113	2.04E-20
3.969	2.26	4.425	5.74E-113	1.88E-20
3.97	2.26	4.425	5.28E-113	1.73E-20
3.971	2.26	4.425	4.86E-113	1.59E-20
3.972	2.26	4.425	4.47E-113	1.46E-20
3.973	2.26	4.425	4.11E-113	1.34E-20
3.974	2.26	4.425	3.78E-113	1.24E-20
3.975	2.26	4.425	3.48E-113	1.14E-20
3.976	2.26	4.425	3.20E-113	1.05E-20
3.977	2.26	4.425	2.95E-113	9.63E-21
3.978	2.26	4.425	2.71E-113	8.86E-21
3.979	2.26	4.425	2.49E-113	8.15E-21
3.98	2.26	4.425	2.29E-113	7.50E-21

3.981	2.26	4.425	2.11E-113	6.90E-21
3.982	2.26	4.425	1.94E-113	6.35E-21
3.983	2.26	4.425	1.79E-113	5.84E-21
3.984	2.26	4.425	1.64E-113	5.37E-21
3.985	2.26	4.425	1.51E-113	4.94E-21
3.986	2.26	4.425	1.39E-113	4.55E-21
3.987	2.26	4.425	1.28E-113	4.19E-21
3.988	2.26	4.425	1.18E-113	3.85E-21
3.989	2.26	4.425	1.08E-113	3.54E-21
3.99	2.26	4.425	9.97E-114	3.26E-21
3.991	2.26	4.425	9.17E-114	3.00E-21
3.992	2.26	4.425	8.44E-114	2.76E-21
3.993	2.26	4.425	7.76E-114	2.54E-21
3.994	2.26	4.43	7.14E-114	2.34E-21
3.995	2.26	4.43	6.57E-114	0.087288
3.996	2.26	4.43	6.05E-114	0.080308
3.997	2.26	4.43	5.56E-114	0.073887
3.998	2.26	4.43	5.12E-114	0.067979
3.999	2.26	4.435	4.71E-114	0.062544
4	2.265	4.435	4.33E-114	0.144831

APPENDIX D